



Pre-treatments of Lithium Foil Surface for Improving the Cycling Life of Li Metal Batteries

Nicolas Delaporte, Yuesheng Wang and Karim Zaghib*

Hydro-Québec, Center of Excellence in Transportation Electrification and Energy Storage, Varennes, QC, Canada

Liquid electrolytes used in Li-ion batteries are flammable and slowly degrade to form a solid electrolyte interface (SEI) that irreversibly consumes lithium, decreasing the Coulombic efficiency of the battery. In addition, lithium anodes undergo severe morphology changes during cycling and Li dendrites are formed, which may cause short circuits inside the battery. Safety concerns and the requirement of higher energy density have stimulated a search for a durable solid-state lithium rechargeable battery (SSLB) with an inorganic or dry polymer electrolyte that is more stable toward the lithium metal and suppresses the growth of lithium dendrites. Reducing the reactivity and increasing the poor contact between solid interfaces in these all-solid-state batteries remain challenging and Li-surface modification is one option to be explored to remedy these problems. Here, we review recent progress in surface pre-treatment of 2D lithium foil to enhance the electrochemical performance of various battery configurations. The review is organized based on the different types of modification reported in the literature.

Keywords: lithium, solid state batteries, treatment, anode, surface

OPEN ACCESS

Edited by:

Piercarlo Mustarelli,
University of Milano Bicocca, Italy

Reviewed by:

Guosheng Li,
Pacific Northwest National Laboratory
(DOE), United States

Yusong Zhu,
Nanjing Tech University, China
Stefania Ferrari,
Università degli Studi G. d'Annunzio
Chieti e Pescara, Italy

*Correspondence:

Karim Zaghib
zaghib.karim@hydro.qc.ca

Specialty section:

This article was submitted to
Energy Materials,
a section of the journal
Frontiers in Materials

Received: 26 July 2019

Accepted: 14 October 2019

Published: 08 November 2019

Citation:

Delaporte N, Wang Y and Zaghib K
(2019) Pre-treatments of Lithium Foil
Surface for Improving the Cycling Life
of Li Metal Batteries.
Front. Mater. 6:267.
doi: 10.3389/fmats.2019.00267

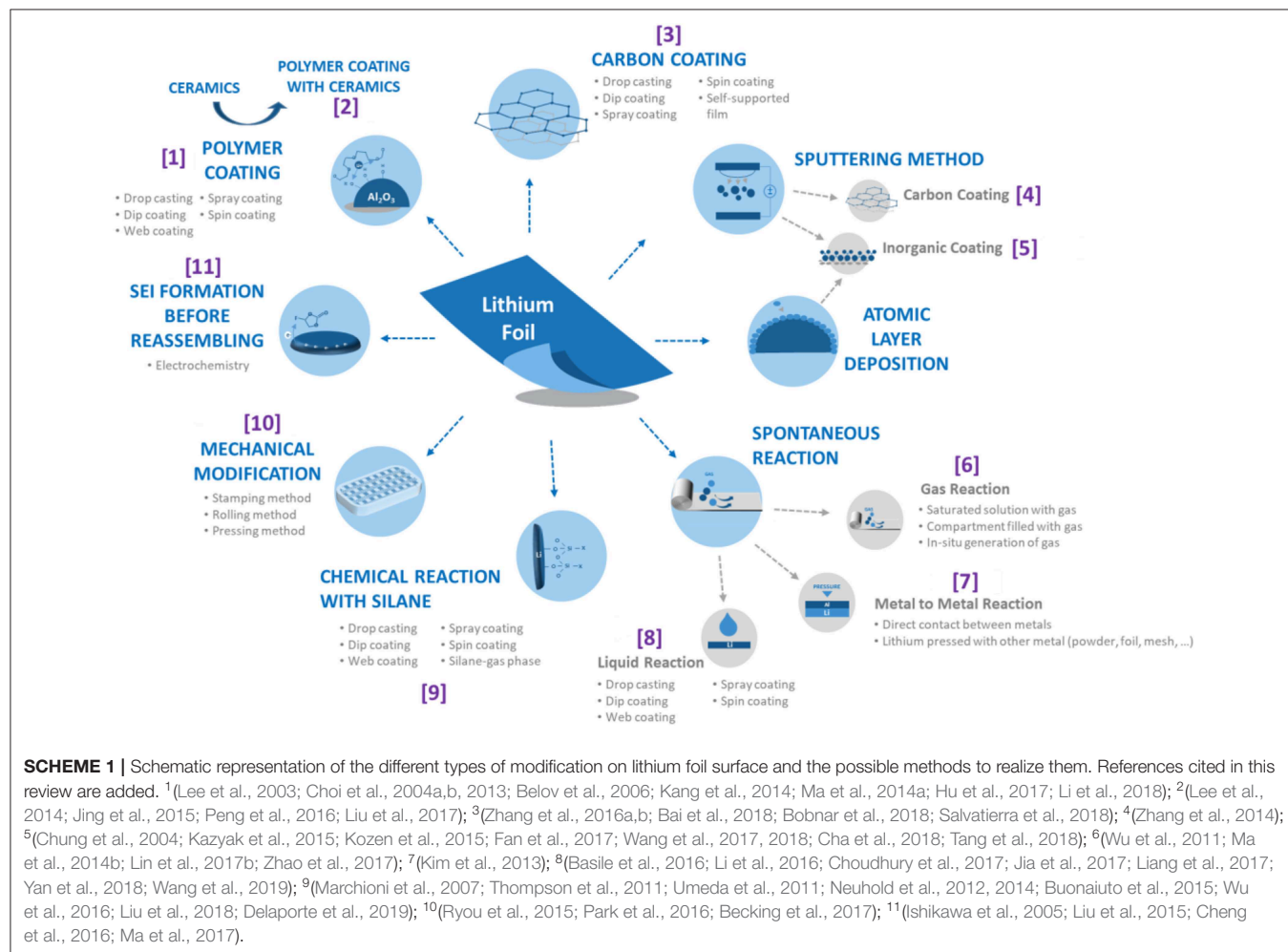
INTRODUCTION

Rechargeable lithium metal batteries have been investigated since the 1980s due to the high theoretical specific capacity (3,860 mAh g⁻¹), low redox potential (-3.04 V vs. SHE), and low gravimetric density (0.534 g cm⁻³) of Li metal (Xu et al., 2014). Unfortunately, using lithium as the anode created a series of issues, such as lithium corrosion, which led to dendrite formation and large volume changes, resulting in a low cycling stability of a few hundreds of cycles (Tarascon and Armand, 2001). Moreover, the high reactivity of lithium has raised safety concerns (Aurbach et al., 2000). Two approaches were proposed to overcome these issues (Lin et al., 2017a). The first approach involved the use of a polymer electrolyte, which is less reactive with lithium as compared to liquid electrolytes, forming a solid-state lithium rechargeable battery (SSLB) (Stone et al., 2012; Zhamu et al., 2012). The second approach was to replace Li metal with another material capable of intercalating Li⁺ ions reversibly at low voltage, leading to the so-called "lithium-ion" lithium rechargeable batteries (Yazami and Touzain, 1983). In 1989, the graphite anode, invented by Yoshino Akira, greatly improved the safety of lithium rechargeable batteries, contributing to the commercial success of Li-ion batteries (Dahn et al., 1990; Fong et al., 1990). Although graphite has been the dominant anode since 1990, it is unable to meet the demand for high energy storage. This aspect has reignited research interest in the use of lithium metal as an anode (Akridge and Vourlis, 1986; Agrawal and Pandey, 2008). SSLBs are of great interest due to their high gravimetric and volumetric energy densities, wide operable temperature range, and high safety in comparison to traditional liquid electrolyte-based systems (Notten et al., 2007). However, fundamental issues

of SSLB remain unresolved, particularly in the area of electrochemical interfaces (Kim et al., 2011). Reactivity of lithium with some ceramic electrolytes (e.g., LAGP), poor adhesion at the Li–electrolyte interface, and dendrite growth are some major problems to address (Odzimek and Irish, 1992; Sudo et al., 2014). Many strategies, such as using super-concentrated electrolytes; electrolyte additives based on fluorinated, nitrogenous, and polysulfide compounds; artificial solid electrolyte interphase (SEI) structures; separator modification with metal-organic frameworks; and nano-carbon or anode structures for hosting Li metal, have been demonstrated to be effective in improving the efficiency and cycle life of Li metal electrodes (Odzimek and Irish, 1993; Li et al., 2001; Bouchet, 2014; Zheng et al., 2014; Fu et al., 2017; Paoletta et al., 2019). However, most of these strategies are not transposable to the industrial scale because of practical or economic reasons, or are simply not adapted for SSLB technology. For these reasons, they are not mentioned in this paper.

The focus of this review is limited to the surface pre-treatment of lithium metal foil for Li metal batteries. That is organized based on the different types of modification reported in the literature and that we found potentially interesting for large-scale production of modified or protected lithium electrode (see

Scheme 1 for structure of review). In a first section, we introduce the polymer coating (with and without fillers) on lithium that acts as a physical barrier to impede Li dendrites progression and to accommodate volume change during Li stripping/plating cycles. A second section is focalized on deposition of carbon and spontaneous reduction of carbon on lithium surface to provide an intermediate 3D host structure for lithium storage (between lithium surface and electrolyte). The third part is dedicated to nanometric ceramic coating made by sputtering and atomic layer deposition (ALD) methods, which bring a compact and homogeneous barrier between Li metal and electrolyte without affecting Li^+ conduction. Then, we encompassed in a same section what we call spontaneous chemical reactions that include gas, liquid, and metal-to-metal reactions. These reactions exploit the highly reductive potential of lithium metal to spontaneously generate metal alloys and inorganic and/or organic layers on its surface. The surface grafting of silane species, which is also a spontaneous reaction, has been widely investigated in the past and is thus presented in an individual section. Another part presents the mechanical modification of lithium, which is known to be a highly deformable metal under pressure. The stamping technique allows to increase the active surface area of lithium and permits to create hot spots for lithium deposition limiting the



formation of dendrites. The last section, entitled *SEI formation before reassembling*, reports surface modifications of lithium foil directly performed by electrochemistry in a cell. We believe that this review will provide readers with a deep understanding of lithium surface modification in the development of novel methods for solid-state batteries.

Polymer Coating on Lithium Foil

One of the easiest and industrially transposable method for surface protection of lithium is to coat a polymer or polymer/Li salt mixture on its surface via spray or dip coating, with the help of a spin coater or employing the so-called doctor blading method. The polymer chosen has to be stable with lithium and ionically conductive at low temperature. In a way, the polymer layer deposited on the lithium surface should be comparable to common solid polymer electrolytes (SPEs) generally reported in the literature, which should have a low T_g to remain rubbery at ambient temperature to preserve a Li^+ conductivity similar to that of the liquid electrolyte system. To accommodate the lithium deformation during cycling and especially to avoid Li dendrite formation, the polymer needs to present a good flexibility and should be characterized by a high Young's modulus.

Li et al. (2018) proposed a smart SEI layer with high elasticity to accommodate the large volume change during Li plating/stripping. Li polyacrylic acid (LiPAA) was selected as a polymer for its remarkably high stretchability (582% strain to its initial length) and its ability to form a uniform ionic conducting surface coating. A 20-nm-thick layer of lithiated polymer was formed on the Li surface by drop casting of a DMSO solution containing polyacrylic acid. The interfacial stability of this coated Li foil was first evaluated in a symmetrical cell and revealed a superior long-term cycling performance characteristic of stable Li plating/stripping. While the Li/Li symmetrical cell showed important voltage fluctuations after only 83 and 70 cycles at 0.5 and 1 mA cm^{-2} , the LiPAA-Li/LiPAA-Li cell presented flat voltage plateaus for up to 700 h at 0.5 mA cm^{-2} . Moreover, the authors showed that the capacity of a $\text{LiNi}_{1/3}\text{Co}_{1/3}\text{Mn}_{1/3}\text{O}_2$ cathode of high area capacity (3.4 mAh cm^{-2}) cycled with unmodified lithium started to decay after only 20 cycles, while it remained stable for at least 40 cycles when the LiPAA-Li was utilized. Another ionically conductive polymer was proposed by Choi et al. (2013). They also prepared a DMSO solution of a co-polymer spread by spin-coating directly on the lithium foil surface. An homogeneous, thin poly(vinylene carbonate-co-acrylonitrile) [P(VC-co-AN)] layer of ~ 150 nm of thickness was obtained. LiCoO_2/Li cells were assembled, and after 100 cycles at a $C/2$ rate, ~ 76 and 91% of the initial discharge capacity was obtained when the unmodified and coated Li were employed, respectively. These results were ascribed to the suppression of lithium corrosion due to the absence of direct contact with the electrolyte and also to the inhibition of dendrite formation during cycling as confirmed by SEM analyses of aged electrodes. Another research group reported the cross-linking reaction under UV assistance of poly(ethylene glycol) dimethacrylate polymer in the presence of a photoinitiator (Lee et al., 2003). The tough polymer layer of ~ 10 μm was found to be useful to reduce the migration of polysulfides from the

cathode to the Li anode in lithium/sulfur batteries. In fact, the cell assembled with the standard liquid electrolyte showed a stable discharge capacity of 270 mAh g^{-1} for up to 100 cycles, which was attributed to the formation of a stable SEI. Moreover, an overcharge phenomenon was observed around 2.5 V when uncoated Li was used, due to the reaction of polysulfides with the Li anode. This reaction was efficiently suppressed with the polymer layer coated on the Li surface. These results were also demonstrated for lithium coated with a 10- μm -thick layer of PEDOT-co-PEG polymer (Ma et al., 2014a). The lithium foil was immersed five times in a strongly diluted nitromethane solution containing the polymer and subsequently dried to obtain a sufficiently thick layer. A clear improvement was observed for long cycling experiments at 0.2C since ~ 876 mAh g^{-1} was obtained after 200 cycles corresponding to a capacity retention of 73.5%. The Li-S battery assembled with the as-received lithium only delivered 400 mAh g^{-1} , which corresponded to 33% of the initial discharge capacity. SEM analyses after cycling showed serious corrosion at the surface of the unmodified lithium with a $\text{Li}_2\text{S}/\text{Li}_2\text{S}_2$ layer of more than 100 μm , while only 40 μm was observed for the polymer-coated lithium. The shuttle effect and dendrite growth at the lithium surface were found to be effectively suppressed, resulting in excellent stability and better Coulombic efficiency. Another research group also tested the effect of a PEDOT-co-PEG polymer layer on the lithium surface, but this time investigating the electrochemical performance of LiCoO_2 -Li batteries (Kang et al., 2014). The surface coverage was realized by spin-coating, giving a thinner thickness than the dipping method and a layer of ~ 380 nm was obtained. Li/electrolyte/Li symmetric cells assembled with fresh lithium showed a progressive increase in internal resistance (R_{SEI} and R_{CT}) with time (10 days), while the AC impedance spectra remained unchanged for polymer-coated lithium. These results indicate the suppression of deleterious reactions between lithium and the electrolyte due to the absence of direct contact. It was also confirmed with a long-term cycling experiment at 0.5C of LiCoO_2 -Li batteries. After 200 cycles, 87.3 and 9.3% of the initial discharge capacity were obtained for cells assembled with modified and pristine Li, respectively. SEM analyses of coated lithium after cycling showed a smooth, flat surface absent of the dendritic morphology usually observed for pristine lithium anodes. The enhanced electrochemical performance was attributed to the stabilization of the SEI, suppression of electrolyte degradation, and dendrite growth during cycling. An interesting method consisting of direct acetylene polymerization on lithium metal surface was proposed by Belov et al. (2006). A catalyst solution was cast on lithium foil followed by the injection of purified acetylene gas to initiate the polymerization. The thickness of the polyacetylene film (PA) was easily controlled by reaction time and gas pressure. The effect of a thin PA film on lithium anode was evaluated in a coin-cell with a LiCoO_2 cathode and a Celgard[®]-type separator. After few formation cycles, electrochemical impedance spectroscopy measurements showed lower electrolyte (R_{el}) and charge-transfer (R_{CT}) resistances when the modified Li was utilized. R_{el} values of 3 and 25, and R_{CT} values of 40 and 380 Ω were obtained with PA-coated and fresh lithium anodes, respectively. The authors claim that this

layer can effectively protect the lithium during cycling, resulting in better cell impedance and long cycling life. A stable SEI layer was achieved by *in situ* polymerization of ethyl α -cyanoacrylate (ECA) in the presence of LiNO_3 salt (Hu et al., 2017). LiNO_3 and ECA monomers are properly dissolved in acetone and spread on the lithium surface using a 200- μm doctor blade and let to dry under an argon flow in a glove box. Polymerization is initiated by hydroxyl groups present on the lithium surface. A symmetric cell with modified lithium electrodes showed stable Li stripping/plating for more than 200 cycles while that assembled with pristine lithium presented higher overvoltage and short-circuited after only 100 cycles at 1 mA cm^{-2} . Additionally, the modified lithium was also tested in a long cycling experiment at a 2C rate with a LiFePO_4 cathode. Capacity retention of 5 and 93% after 500 cycles at 2C was obtained with pristine and modified lithium anodes, respectively. Interestingly, it was demonstrated by X-ray photoelectron spectroscopy that the reaction between cyano groups in ECA and NO_3^- from LiNO_3 with the lithium surface led to a uniform inorganic nitrogenous interface layer. This layer remained intact even after 150 cycles in the $\text{LiFePO}_4/\text{Li}$ battery and protected the lithium from side reactions with the electrolyte and impeded the formation of dendrites. Choi et al. (2004a) reported a semi-interpenetrating network (IPN) structure for the protection of lithium electrodes made by the ultraviolet radiation-curing method. A copolymer solution of Kynar 2801 was mixed with a curable monomer (1,6-hexanediol diacrylate), a liquid electrolyte, and a photoinitiator, and spread on lithium before irradiation under UV light. The IPN structure of 3.5 μm suppressed the dendritic lithium formation and reduced the growth of an SEI layer formed by decomposition of organic solvents and salt anions in the LiCoO_2/Li cells. Consequently, the electrochemical performance for the battery assembled with the modified lithium remained quite stable upon cycling at C/2 for 100 cycles with a capacity retention of 80%. By contrast, the bare lithium, after 20 cycles, only 70% of the initial discharge capacity was obtained, which dramatically decreased on subsequent cycles and the battery was not able to cycle for more than 40 cycles. The same research group further investigated the effect of the incorporation in the polymer mixture of an anion receptor (Choi et al., 2004b). Oligo(ethylene glycol) borate (OEGB) (an anion receptor) was first synthesized by a simple dehydrocoupling reaction between borane tetrahydrofuran complex and diethylene glycol methyl ether. The addition of an anion receptor in the polymer/Li salt mixture increased the ionic conductivity from $\sim 8.5 \times 10^{-4}$ to $1.1 \times 10^{-3} \text{ S cm}^{-1}$ and improved the lithium transference number (t_{Li}^+) from 0.61 without OEGB to 0.82 when a molar OEGB/ LiClO_4 ratio of 0.7 was used. The Lewis acid–base interaction between the OEGB anion receptor and ClO_4^- anion favors the dissociation of lithium salt and by consequence lowers the interfacial resistance to the lithium metal anode. Furthermore, R_{CT} values of ~ 35 and 25Ω were obtained for LiCoO_2/Li cells assembled with modified lithium with polymer and OEGB-containing polymer, respectively. Finally, the incorporation of this anion receptor also increased the cycle life of the battery and a capacity retention of 85% after 100 cycles at C/2 was obtained.

Inorganic fillers (e.g., Al_2O_3 , TiO_2 , and BaTiO_3) were often mixed with a polymer to yield an organic–inorganic hybrid composite electrolyte. It is generally reported that the incorporation of ceramics in the polymer matrix induces an increase of the ionic conductivity and improves the mechanical properties and the interfacial stability of the polymer electrolyte. In addition, well-dispersed fillers could slow down lithium dendrite progression, and even suppress them. Thus, this strategy is particularly well-adapted for surface modification of lithium leading to a strong barrier against dendrites and avoiding direct contact with liquid electrolyte.

An artificial SEI layer with high mechanical strength, good flexibility, and high Li-ion conductivity was proposed by Liu et al. (2017). A mixture of freshly synthesized Cu_3N sub-100-nm spherical particles and styrene butadiene rubber copolymer (SBR) was deposited on the Li surface via doctor blade casting. In contact with lithium foil, Cu_3N is converted to a highly Li-ion conducting Li_3N phase, which is strongly attached to lithium due to the polymeric matrix. Coulombic efficiencies of bare Cu and Cu foil protected with a similar polymer matrix were compared in a standard carbonate-based electrolyte. For bare Cu, the Coulombic efficiency started at around 95% and quickly decayed to 70% after 50 stripping/plating cycles due to the growth of Li dendrites and the continuous degradation/formation of the SEI layer. By contrast, for the modified Cu, the Coulombic efficiency remained stable for more than 100 cycles and an average value of 97.4% was obtained. $\text{Li}_4\text{Ti}_5\text{O}_{12}/\text{Li}$ (LTO/Li) cells were also assembled with different lithium metal anodes, and the best electrochemical performances were obtained for $\text{Cu}_3\text{N}+\text{SBR}$ protected porous lithium. The battery assembled with a 50- μm -thick Li foil started to decay after 20 cycles and presented a Coulombic efficiency of 88.3%. With protected lithium, the LTO/Li cell was able to cycle for at least 90 cycles with a Coulombic efficiency of 97.4%. The amelioration of electrochemical performances was associated with the synergic effect between the inorganic nanoparticles and the polymeric binder. The closely packed Li_3N filler suppressed the dendrite growth while the polymer matrix maintained the integrity of the film, avoiding cracking during cycling. Moreover, the high Li-ion conductivity of the Li_3N layer guaranteed uniform Li-ion flux across the whole electrode that reduced the risk of dendrite formation. A composite protective layer (CPL) made of Al_2O_3 particles (1.7 μm of average diameter) and polyvinylidene fluoride-hexafluoro propylene (PVDF-HFP) deposited on the lithium surface was investigated to enhance the cycle life of Li-oxygen batteries (Lee et al., 2014). A layer $\sim 20 \mu\text{m}$ in thickness clearly had a positive impact on the cycling performances of Co_3O_4 -Super P/Li batteries. The cell with the CPL-coated lithium electrode maintained a discharge capacity of 1,000 $\text{mAh g}_{\text{carbon}}^{-1}$ for 80 cycles ($I = 0.1 \text{ mA cm}^{-2}$, fixed capacity = 1,000 $\text{mAh g}_{\text{carbon}}^{-1}$) while that with pristine Li showed a rapid capacity reduction with cycles and during the 40th cycle the discharge voltage dropped to the terminal voltage of 2.2 V before reaching the fixed capacity. At the 80th cycle, only 320 $\text{mAh g}_{\text{carbon}}^{-1}$ was obtained. SEM investigations showed the formation of mossy lithium after cycling when no surface treatment was performed. Contrastingly, the surface of the CPL-coated lithium was quite

smooth, confirming the effective suppression of electrolyte decomposition as well as the protection of lithium from oxidation caused by O_2 diffusion through the bulk electrolyte. The effect of similarly modified lithium was studied by Jing et al. (2015), although the focus was improvement of lithium-sulfur batteries. In this example, 100-nm Al_2O_3 spheres were utilized with PVDF as a binder and the mixture prepared in DMF solvent was spread by spin-coating on lithium foil. Cross-sectional SEM images showed porous Al_2O_3 layers of a few micrometers depending on preparation conditions, which are considered efficient to provide a pathway for electrolyte penetration and impede the direct contact of polysulfides with lithium anode. In fact, after 50 charge/discharge cycles, the surface of pristine lithium appeared loose with serious cracks, and chemical mapping revealed high amounts of sulfur deposition. The surface of modified lithium remained as smooth as before cycling with only trace S deposition. The S/Li cells assembled with the pristine and the polymer-coated lithium anodes gave a capacity retention of 50 and 70% after 50 cycles, respectively. In conclusion, side reactions between Li and soluble polysulfides are suppressed during cycling, ensuring better electrochemical performance. A porous polyimide layer (PI) with Al_2O_3 filler (particle size ~ 10 nm) providing inter-space to confine lithium growth was proposed by Peng et al. (2016). A Li/Li symmetric cell assembled with unmodified lithium electrodes only cycled for 8 h within a voltage window of ± 0.5 V and a current density of 2.125 mA cm^{-2} before reaching the voltage limit. Additionally, due to the large consumption and degradation of the electrolyte, the R_{CT} reached 120Ω cm^{-2} at the end of the test. With the PI-coated lithium, the system was able to work for more than 160 h (20 times longer) and presented a stable R_{CT} with a plateau at $\sim 8 \Omega$ cm^{-2} for roughly 140 h and attained 18Ω cm^{-2} after 160 h. Cu/LiFePO₄ cells were tested to further demonstrate the utility of the Al_2O_3 -polyimide layer to inhibit dendrite formation and electrolyte degradation. The porous layer was also deposited on Cu foil, and the cells were tested under a C/5 rate between 3 and 4 V. The protected Cu/LiFePO₄ cell showed a Coulombic efficiency of 74.5% for the first cycle, which stabilized to 97.5% for the 50 subsequent cycles. Due to the limited amount of lithium in this electrode configuration, the discharge capacities slowly dropped from 112.1 (1st cycle) to 111.6, 95.6 and 33.6 mAh g^{-1} at the 20th, 30th, and 50th cycle, respectively. In contrast with the bare Cu, the capacity decreased from 151.3 to 30.6 mAh g^{-1} during the first charge/discharge cycle and reached only 4.1 mAh g^{-1} in the 3rd cycle.

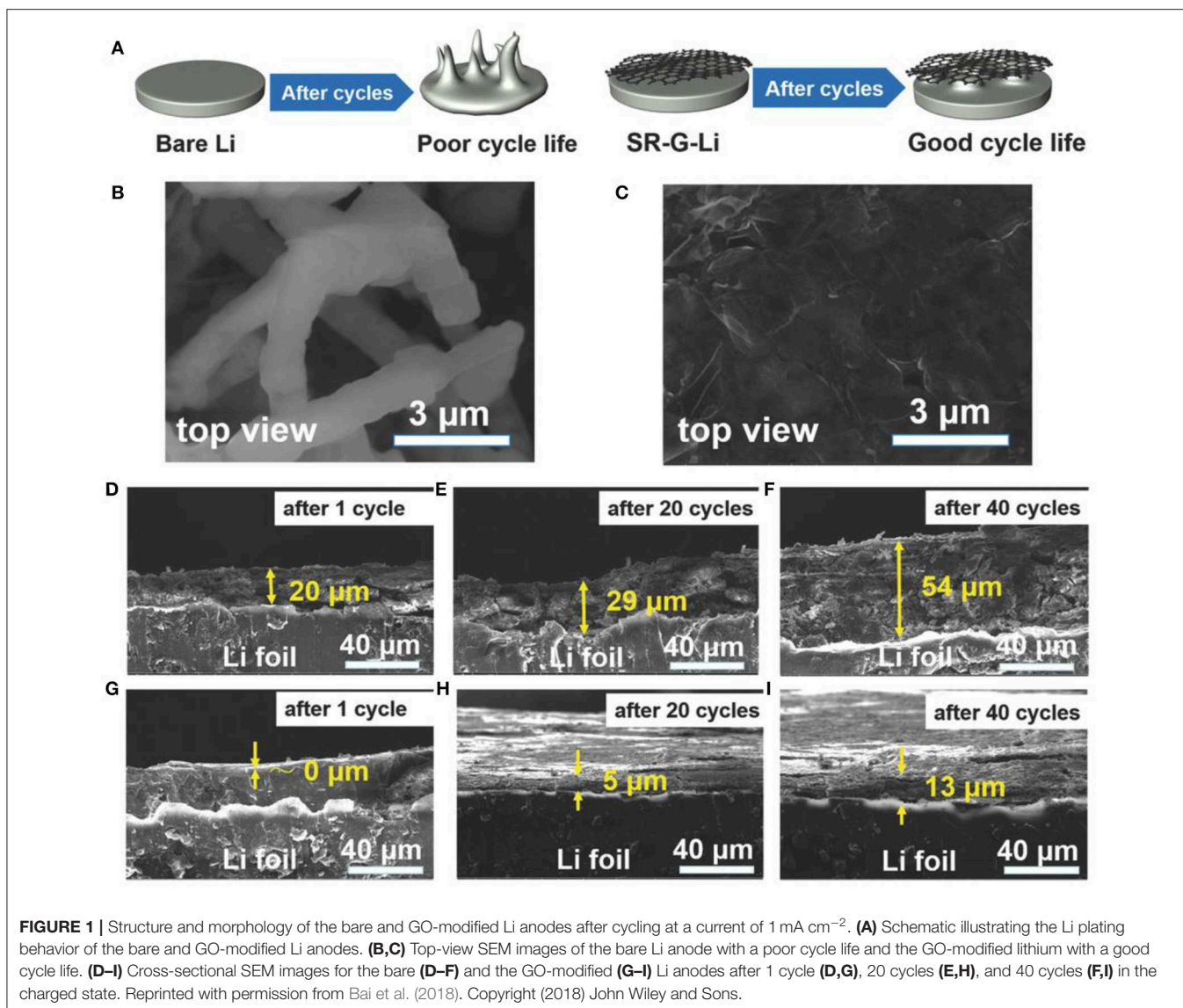
Carbon Coating

Carbon coating on lithium surface can be useful for many reasons. Firstly, this material and especially graphitic carbons (e.g., graphite) have the ability to store Li^+ ions and thus artificially increase the specific surface area of the lithium foil. Secondly, its layered structure can adjust to the volumetric change during repeated stripping/plating cycles. Then, since the compact structure of graphitic carbons, the direct contact between electrolyte and lithium is avoided, limiting side reactions and electrolyte consumption. Finally, the mechanical flexibility of carbon sheets is supposed to reduce the Li dendrite

growth. In consequence, graphitic carbons may be useful to favor homogeneous lithium electrodeposition (increase of active surface area and diminution of actual current density) in addition to avoiding dendrite progression through the electrolyte.

A simple, scalable spray-painting method was successfully developed to achieve the surface modification of lithium foil by spontaneous reduction of a THF solution containing graphene oxide (GO) (Bai et al., 2018). Bare Li/Li symmetric coin cells displayed random large voltage oscillations during the first 100 cycles, indicating the formation of an unstable Li/electrolyte interface as well as dendrites leading to internal short circuit. By contrast, the cycling for GO-modified Li electrodes showed a stable charge/discharge plateau for more than 1,000 cycles. It is important to note that this cycling has one of the longest lifespans reported with standard carbonate-based electrolytes. Cross-sectional SEM images of bare lithium after 20 and 40 cycles (presented in Figure 1) revealed that the Li-dendrite layers have increased by 45 and 170%, respectively, while the modified Li presented a small percentage increase after 40 cycles. Finally, LiFePO₄/Li batteries presented a capacity retention of 69 and 99% after 300 charge/discharge cycles at 1C, when unmodified and GO-coated lithium were used, respectively. Similarly, Bobnar et al. (2018) reported the modification of lithium foil with fluorinated reduced graphene oxide (FG) by drop casting a propylene carbonate solution of FG. The FG layer on the lithium anode serves as an interlayer that prevents the formation of dendrites and its effect was investigated with LiFePO₄ and sulfur cathodes. Unfortunately, only results with FG-Li anode were presented and not compared with the bare lithium. Thus, a capacity retention of 81% was observed after 250 charge/discharge cycles at a 1C rate for the LFP/Li battery. For the Li/S battery, we calculated a capacity retention of 53% over 100 cycles at C/5 in 1 M LiTFSI TEGDME:DOL (1:1) electrolyte. Another research group studied the effect of solvents (ethanol, acetonitrile, ether, and DMC) on the dispersion efficacy of GO powder and its impact on the formation of uniform strong passivation film on the lithium surface (Zhang et al., 2016a). The Li/Li symmetric cell assembled with pure lithium showed erratic voltage response while the GO-Li/GO-Li cell presented stable stripping/plating plateaus over 600 h. This enhancement is due to the limitation of dendrite formation and the side reaction between metallic Li and the electrolyte, which is confirmed by XPS analysis. Long-cycling experiments at C/10 of Li/S batteries demonstrated the protective role of the GO layer toward the corrosion induced on the lithium surface by polysulfides formed in the electrolyte. The capacity of the pure Li/S battery decreased from 840 to 487 mAh g^{-1} after 200 cycles while that for the GO-Li/S cell reached 707 mAh g^{-1} at the end of experiment.

A slightly different strategy from the aforementioned research consists of the formation by filtration method of a self-standing GO film that will be further applied on a lithium surface as a strong barrier against dendrite formation (Zhang et al., 2016b). Voltage vs. times profiles for pure and GO-Li electrodes in symmetric cells were studied. The haphazard changes in the charge/discharge cycles for pristine lithium were ascribed to dendrite formation. Compared to GO-Li electrodes, a stable voltage was observed over 600 h (100 cycles). The Coulombic



efficiency of the GO-Li/Cu cell remained stable at 90% after 100 cycles while that of pristine-Li/Cu dropped to 70% after only 40 cycles and completely vanished after 50 cycles due to an internal short circuit. On one hand, the mechanical flexibility of GO sheets is helpful in suppressing Li dendrite growth, and on the other hand, the layered structure of the GO film provided lithium storage space and can adjust to the volumetric change during repeated stripping/plating cycles. The same method was utilized by Salvatierra et al. (2018) to protect lithium metal, but in this case, a self-standing film composed of multiwall carbon nanotubes (MWCNT) was proposed. The physical contact between Li and the MWCNT film gives rise to a spontaneous reduction in nanotubes counterbalanced by the intercalation of Li^+ ions. The lithiation was completed in <30 min and visualized by a color change in the self-standing film from black to red. Li/Li symmetric cells assembled with the MWCNT-Li showed a stable cycling performance for 2,000 h (or 500 cycles) with constant polarization of ~ 20 mV

while the unprotected Li anode presented higher polarization with more oscillatory/peaking behavior. After more than 580 stripping/plating cycles, the modified lithium showed a smooth surface with MWCNTs still visible, while the bare lithium presented a roughened surface covered by Li dendrites. Bare and modified Li were also tested with a sulfurized sulfur cathode (SC) and a capacity retention of ~ 90 and 97% was obtained after 70 cycles at a constant current of $C/2.5$ when the fresh and MWCNT-Li were utilized, respectively.

An amorphous carbon film (a-C) was deposited on the lithium surface by magnetron sputtering with the help of a graphite target (Zhang et al., 2014). The surface was quite compact and uniform and the carbon thickness depended on deposition time (between 50 and 110 nm). The cycling efficiency over 50 cycles for the modified lithium electrode was maintained above 80%, while that for pristine lithium reached a meager 40%. There is clear evidence that the a-C coating on Li foil can prevent the direct contact between the lithium surface and the electrolyte suppressing the

dendrite formation and the formation of a resistive layer, which was confirmed by the invariance in R_{CT} for the symmetric cell standing for 2 days. Unfortunately, the authors did not present electrochemical results of modified lithium with a conventional cathode such as sulfur or LiFePO_4 to clearly show the positive impact of this modification method.

Inorganic Coating

As demonstrated with a-C deposition, the sputtering method is particularly well-adapted to the formation of inorganic coating on a lithium surface. For example, a 10-nm-thick layer of two-dimensional molybdenum disulfide (2D MoS_2) was deposited uniformly on lithium foil with this technique (Cha et al., 2018). The layer was electrochemically lithiated, yielding a flake-like morphology, and this Li- MoS_2 -coated lithium was tested in a battery. First, the Li deposition/dissolution for both types of Li electrode was examined in a symmetric cell. Although the voltage profile was similar at the beginning of the experiment for the two lithium electrodes, after 120 h, a sudden increase in polarization of the bare lithium was observed and attributed to the formation of “dead” Li. By contrast, the Li- MoS_2 -coated lithium maintained a stable voltage polarization of ~ 52 mV over 300 h. Sulfur batteries assembled with both modified and bare lithium electrodes were cycled for 300 cycles at a C/10 rate. A specific capacity of $\sim 1,800$ mAh g^{-1} was obtained for the two cell configurations during the first cycle. However, the pristine Li/S battery showed a continuous decrease in specific discharge capacity at up to 150 cycles and the experiment was prematurely terminated. With the Li- MoS_2 -coated lithium anode, the cell exhibited stable cycling for over 300 cycles with a specific capacity retention of 67%. More interesting, the same battery cycled at C/2, delivered a capacity of ~ 940 mAh g^{-1} after 1,200 cycles and a capacity retention of 84%.

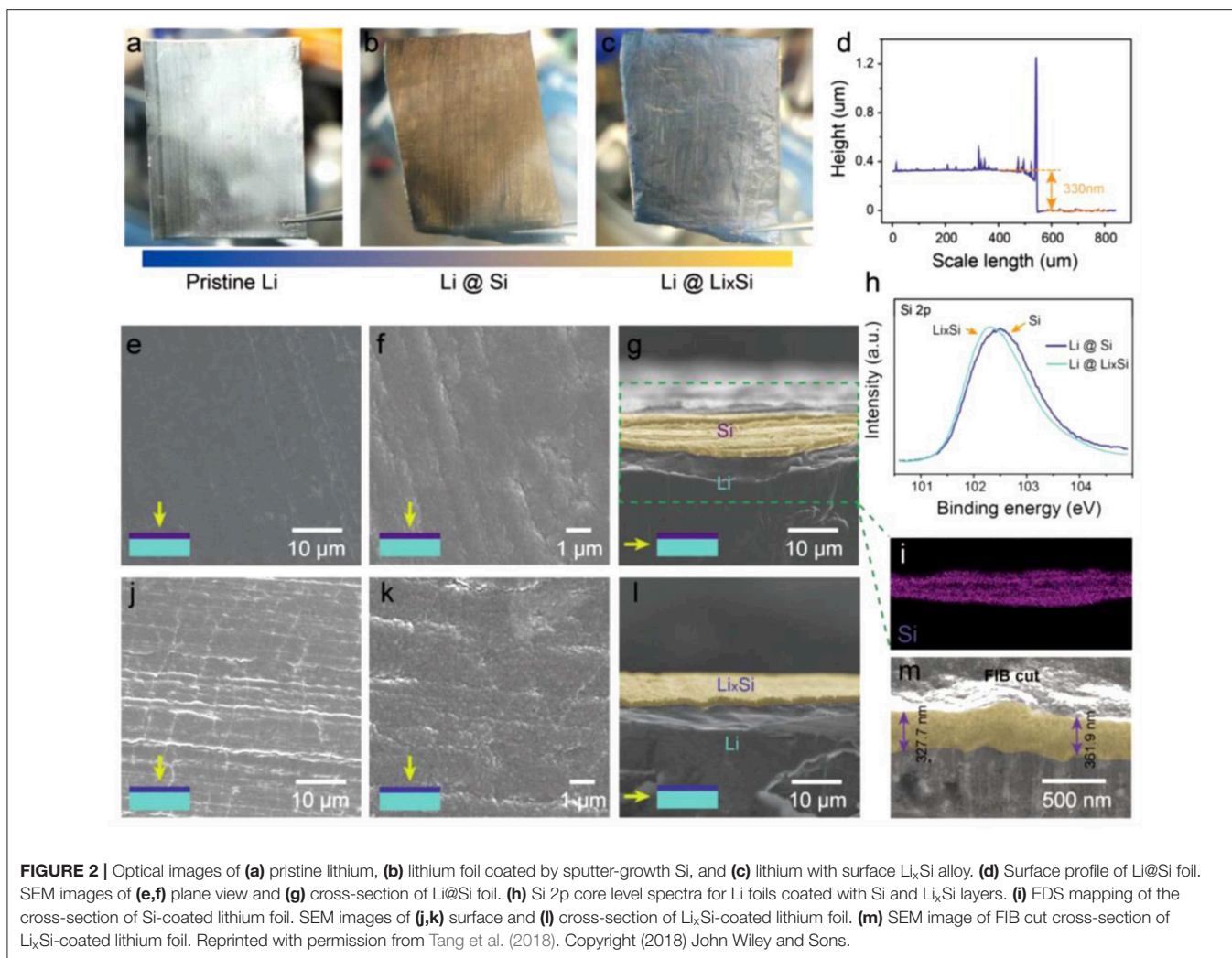
Another research group proposed depositing a Li_3PO_4 film of 30 nm on lithium with the same method (Wang et al., 2017). First, to easily demonstrate the protective role of Li_3PO_4 film, pristine and modified lithium are exposed to air for 1 h. In a few seconds the bare lithium foil became black, while after 1 min, the Li_3PO_4 -modified electrode remained shiny, confirming the compactness of the Li_3PO_4 film. The stability of both modified and unmodified lithium electrodes was evaluated in a Li/Li symmetric cell configuration. After 400 h of charge/discharge cycles at 0.5 mA cm^{-2} , the cell assembled with bare lithium electrodes short-circuited while the one with Li_3PO_4 -modified Li electrodes demonstrated stable cycling for up to 900 h. Thus, the 30-nm amorphous Li_3PO_4 layer can sufficiently and effectively restrain Li dendrite growth. Li/S batteries were also assembled and cycled at a rate of C/2 for 200 cycles. At the end of the experiment, discharge capacities of 486 and 247 mAh g^{-1} were obtained for modified and pristine Li, respectively, which corresponded to a capacity retention of 52 and 28%. Additionally, an average Coulombic efficiency of 89% was calculated for Li_3PO_4 -modified Li and only 84% for the bare lithium. Chung et al. (2004) used the same sputtering method with a Li_3PO_4 target but this time in a nitrogen atmosphere to form *in situ* a lithium phosphorous oxynitride (LiPON) film of ~ 950 nm on the lithium surface. Li stripping/plating experiments showed less polarization at a high cycling rate (10 mA cm^{-2}) and stable cycling for the symmetrical

cell assembled with LiPON-modified Li electrodes. After 50 cycles, electrochemical impedance spectroscopy measurements showed lower R_{CT} (~ 500 Ω cm^{-2}) for the modified lithium in comparison to the bare ($\sim 1,750$ Ω cm^{-2}). Hence, the deposited layer acts as an efficient barrier against electrolyte decomposition and efficiently impedes the formation of an insulating layer. Unfortunately, this lithium was not tested in a full cell with a standard cathode.

A Li^+ ion-conducting layer consisting of an alloy between Li and Si metals (Li_xSi) was recently proposed by Tang et al. (2018). The procedure is specific and requires two steps in which the first consists of the depositing a thin layer of silicon by sputtering followed by a heat treatment at 250°C to form the Li_xSi layer (see **Figure 2** for optical images of modified-lithium foils). When Si is deposited on the lithium, the silvery Li foil changed to yellow, and after heating, a gray color was obtained, confirming the lithiation of silicon. A handmade Li/Li symmetric cell was assembled to follow the voltage profiles and morphological evolutions of the Li electrode during constant deposition of lithium at 1 mA cm^{-2} . For the pristine lithium, the deposition was uneven and porous with the appearance of dendrite after 6 h. By contrast, the modified lithium deposition was smooth and dense even after 10 h of charging. A symmetrical cell with Li_xSi -modified Li electrodes presented a low overpotential of 40 mV with a flat voltage plateau during 200 stripping/plating cycles at 1 mA cm^{-2} while the coin cell assembled with pristine lithium electrodes short-circuited after 156 cycles. The modified lithium was also tested with sulfur and LiFePO_4 cathodes. For instance, when paired with a LiFePO_4 cathode, the cell was able to deliver ~ 136 mAh g^{-1} with almost 100% capacity retention after 350 cycles at a 2C rate while the discharge capacity for the cell assembled with unmodified lithium suddenly decreased after 250 cycles to reach < 60 mAh g^{-1} at the end of the experiment.

Above, we discussed the interest in thin Al_2O_3 coatings to provide inter-space to confine lithium dendrite growth. In a recent study, a research group reported the surface modification of lithium foil with a nanometer-scale Al_2O_3 layer achieved through the sputtering method to suppress the dendrite growth (Wang et al., 2018). Both modified and bare lithium electrodes were cycled in Li/Li symmetric cells at 50°C with a PEO-based polymer electrolyte (LiTFSI salt, EO:Li = 20:1). Impressive enhancement in cycle life was observed when a 20-nm-thick layer of sputtered Al_2O_3 was deposited on Li metal. In fact, constant overvoltage was obtained (~ 40 to 50 mV) over 660 h while the cell constructed with bare lithium electrodes showed a gradual increase in overvoltage (up to 80 mV) before short-circuiting after 550 h of cycling. Additionally, the authors followed the evolution of the overall polarization resistance R_{Overall} as a function of the cycling number and they found that it increased from 91 (1st cycle) to 442 Ω at the 100th cycle for bare lithium. With the Al_2O_3 -modified lithium, the cell presented an increase from 121 to 365 Ω . The authors demonstrated that the thin amorphous film induced a homogeneous lithium nucleation due to a layer-by-layer film growth mode instead of an island growth mode. However, once again, we deplore the absence of electrochemical tests with standard cathodes in this work.

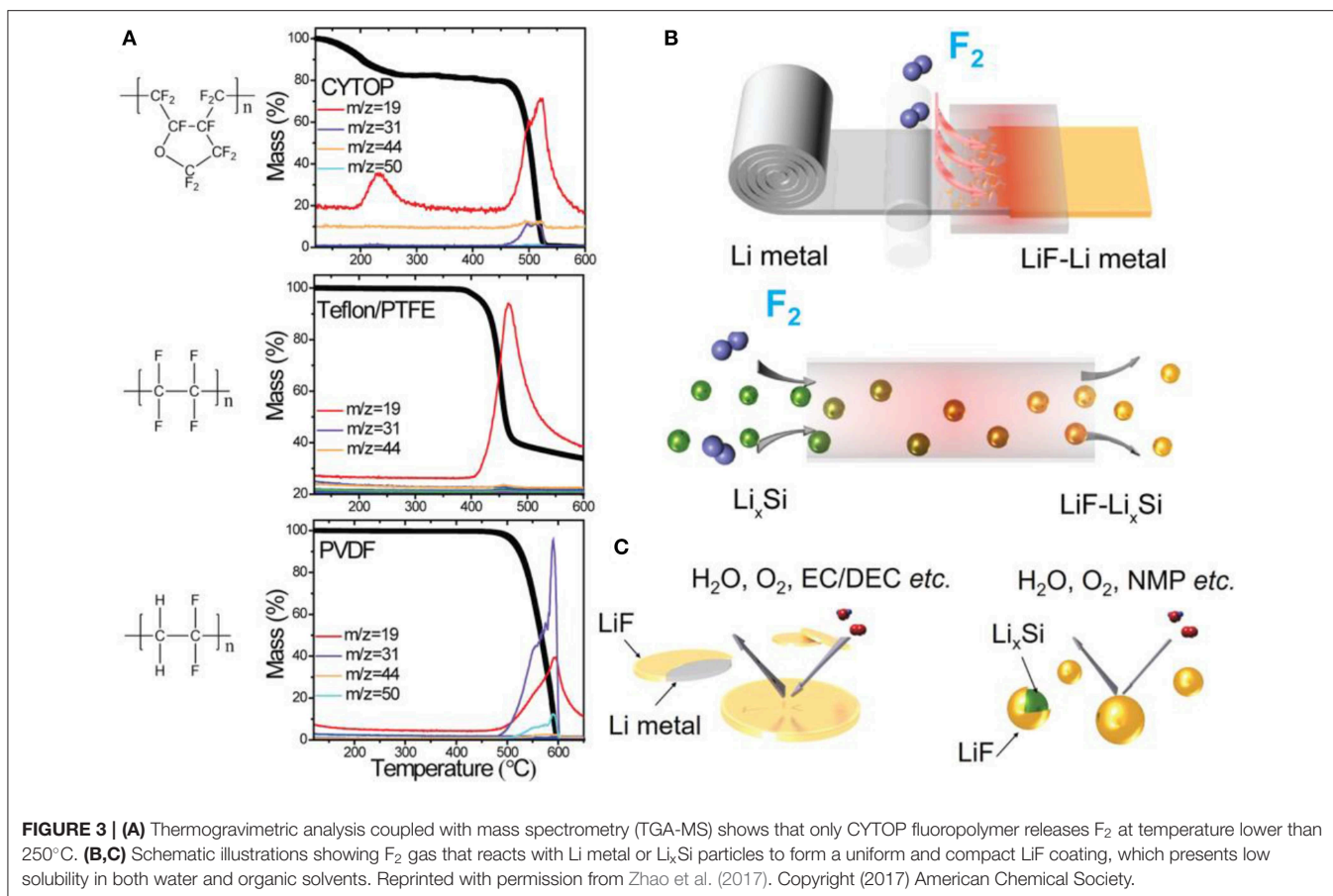
Recently, a LiF layer has been deposited by sputtering on a lithium surface to enhance the lithium electrodeposition and



the cycle life of lithium metal batteries (Fan et al., 2017). Interestingly, the authors demonstrated the preference of Li^+ ions for electrodeposition on Li metal surface rather than on the LiF -protected Li surface. In this case, they used a copper mesh on the Li surface before LiF deposition, and after they removed it, the patterned LiF -coated and the lithium electrodes were cycled and observed by SEM. The Coulombic efficiency for Li/Cu cells assembled with both modified and unmodified copper electrodes was calculated. For the modified copper electrode, a Coulombic efficiency of 99% for more than 90 cycles was obtained, which is a particularly high value. The cell with bare lithium demonstrated a gradual decrease in CE after 20 cycles and dropped to 60% after 90 cycles.

Another promising approach for atomically precise modification of the surface and especially of Li foil is ALD. Layer-by-layer deposition of 2- to 4-nm-thick Al_2O_3 coating on lithium was proposed by Kazyak et al. (2015). In this work, Al_2O_3 was chosen for its ability to form a strong passivating surface film and Li-ion conducting LiAlO_x solid electrolyte. A Li/Li symmetric cell with this modified lithium increased the cycling life by 80%. After ~ 600 cycles at 1 mA cm^{-2}

with bare lithium electrodes, a sudden drop in overpotential and erratic voltage behavior was observed, characteristic of formation and subsequent detachment of dendrites. With protected Li, the voltage remained stable up to 1,100 cycles. SEM analyses after 100 cycles still showed a smooth surface for the Al_2O_3 -coated electrode while the pristine lithium surface was rough and textured, resulting from homogeneous Li-ion flux across the electrode/electrolyte interface. Another example of Al_2O_3 coating of lithium via the ALD method was recently published by Kozen et al. (2015). XPS analysis of modified lithium revealed uniform efficient coverage of lithium by Al_2O_3 ($\sim 14 \text{ nm}$) demonstrated by the absence of the Li 1s peak in the corresponding XPS core-level spectrum. Lithium corrosion prevention was studied in three different environments including storage under atmospheric conditions, direct contact with a PC solvent, and with DME solvent containing elemental sulfur. For instance, 5 min after immersion of bare lithium in DME/S solution, a yellow color appeared due to the formation of polysulfides. The same result was obtained after 1 day for the Al_2O_3 -modified lithium. Long-cycling experiments for Li-S batteries constructed with bare and coated lithium electrodes



were realized. Because of side reactions at the surface of the unprotected Li metal, the cell capacity dropped from $1,200$ to 800 mAh g^{-1} after the first 10 cycles with a Coulombic efficiency of 70 and 88% for the first and the second cycle, respectively. With Al_2O_3 -coated lithium, the capacity loss during the first cycles was avoided due to the absence of direct contact between lithium and polysulfides ($\text{CE} > 95\%$). Finally, after 100 charge/discharge cycles, a capacity retention of 90 and 50% was obtained when ALD-protected and bare lithium electrodes were used.

Spontaneous Chemical Reactions

Simple surface modification of lithium can be achieved by direct reaction with gas. For instance, the formation of a LiF layer following reaction of lithium foil at 150°C for 20 h in an atmosphere (0.5 atm) of 1,1,1,2-tetrafluoroethane (Freon R134a) was reported (Lin et al., 2017b). Cross-sectional SEM images showed good uniformity of the LiF film of ~ 40 nm thickness. Unfortunately, the authors did not directly evaluate the electrochemical performance of this LiF-protected lithium but preferred to use a Li-rGO composite on which a LiF film was deposited with the same procedure. This composite was combined with a sulfur cathode and cycled for 100 charges/discharges at a $C/2$ rate. Better capacity retention was obtained for the anode composite (91%) compared to pristine lithium (73%), although in this example, the Coulombic

efficiency was not improved after modification. By chance, Zhao et al. (2017) also reported the modification of lithium surface with a LiF layer. They built a special procedure for lithium fluorination at 175°C by heating a stainless-steel foil covered with a fluoropolymer, namely, CYTOP. Its decomposition at relatively low temperature ($< 250^\circ\text{C}$), see the corresponding thermogravimetric curve in **Figure 3** generates F_2 gas that slowly reacts with lithium to form a LiF layer ~ 380 nm thick after 12 h of reaction. XPS analysis revealed the major component as LiF with an extremely low percentage of oxygen and carbon contaminants. Two-electrode symmetric cells were assembled with both the modified and bare lithium electrodes. Under a constant current of 1 mA cm^{-2} , the fresh lithium symmetric cell succumbed to anarchic voltage fluctuation after 140 cycles, which was attributed to the desiccation of the electrolyte and dendrite formation. With the LiF-coated lithium, the cell still worked after 300 cycles and presented a constant overvoltage of $\sim \pm 0.15$ V. Full cells with a LiFePO_4 cathode were also tested. Due to the much more stable LiF-coated lithium, the LFP/LiF-coated Li cell exhibited higher discharge capacities at high C-rates than for the LFP/bare Li battery. The protection effect of a LiF layer was further examined in a Li/S battery. The dense LiF coating effectively improved the cycling performance of the cell, since high capacity retention above $1,000 \text{ mAh g}^{-1}$ was obtained after 100 cycles ($\text{CR} = 95\%$). In comparison, the cell assembled with bare lithium exhibited

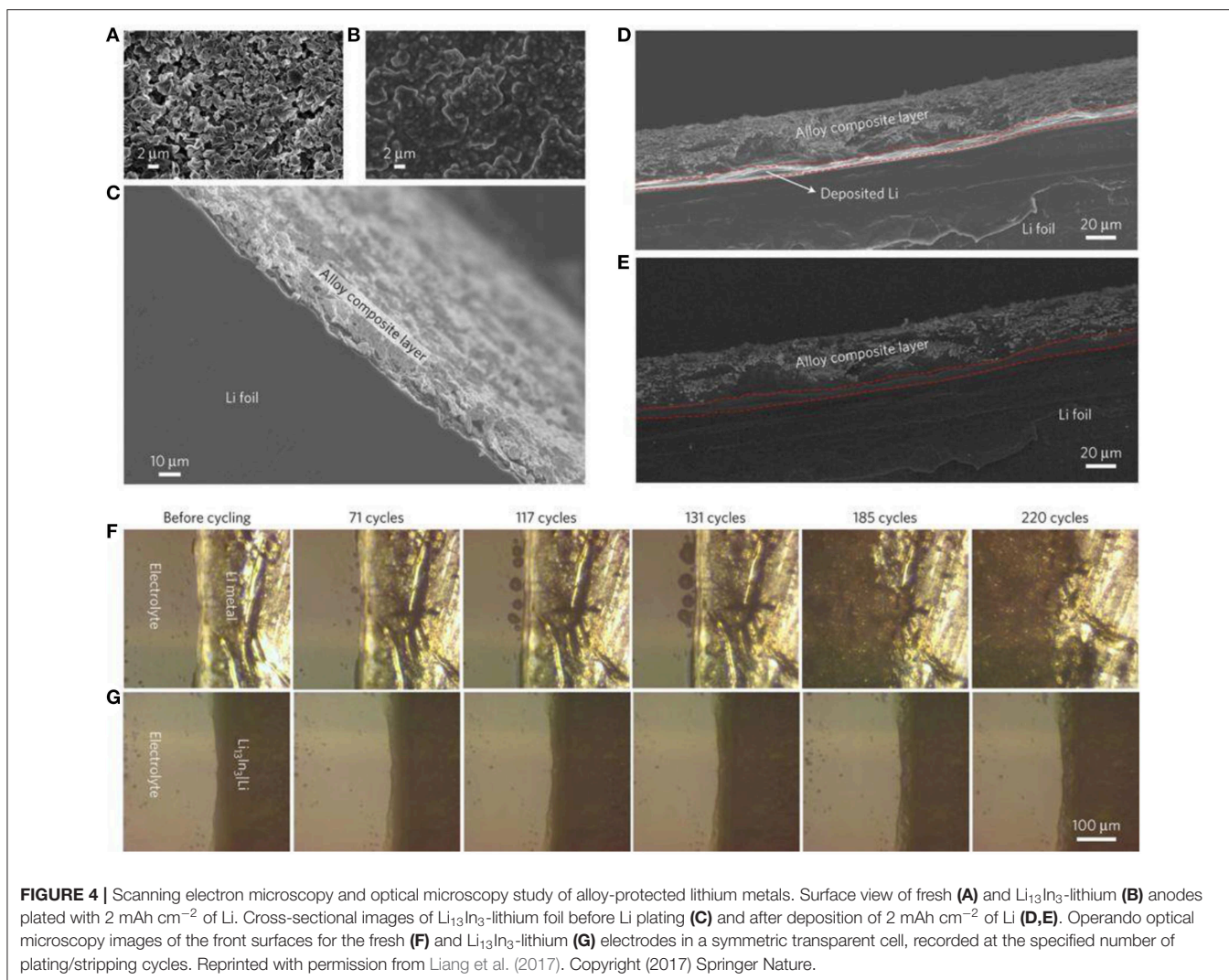
continuous loss of capacity to reach only 900 mAh g⁻¹ at this end of the experiment (CR = 82%).

A simpler method, in which a lithium conductive Li₃N film was successfully deposited on Li metal surface by direct reaction between Li and N₂ gas at room temperature was explored (Wu et al., 2011). XRD analysis revealed only one crystalline phase corresponding to a Li₃N species. The cycling efficiency of both bare and LiF-modified lithium electrodes was compared in a standard carbonated-based electrolyte for 100 cycles. During the first 10 cycles, the Coulombic efficiencies were quite low due to the formation of a Li₂O layer on copper foil, as proposed by the authors. Finally, during the following 90 cycles, a stable Coulombic efficiency of ~89% was obtained for the coated lithium while a standard assemblage presented important fluctuations and gave an average value of only 70%. The enhancement in electrochemical performance was attributed to the protective role of the Li₃N layer against electrolyte corrosion and also to its high ionic conductivity that avoids dendrite formation. Another research group also reported lithium modification with a Li₃N layer (~200–300 nm thick) (Ma et al., 2014b). The authors directly compared the effects of surface modification on Li/S battery performances rather than in symmetric cells. First, the evolution of R_{CT} following storage time at the open circuit voltage (OCV) was compared for the two Li/S cells assembled with bare and coated lithium anodes. The R_{CT} value increased from 59 to 168 Ω after 240 h when the unmodified lithium was used owing to the gradual growth of an SEI layer on the lithium surface. For the Li₃N-protected lithium, the R_{CT} stabilized at 92 Ω after 48 h and remained stable up to 240 h. Additionally, the cycle performance at a C/5 rate and Coulombic efficiencies of the Li/S batteries were compared. After 200 cycles, discharge capacities of 956.6 and 452.2 mAh g⁻¹, corresponding to a capacity retention of 79.7 and 37.2%, were obtained when Li₃N-protected and bare lithium electrodes were used, respectively. Moreover, an average Coulombic efficiency of 91.4% was obtained after modification in comparison to only 80.7% for the blank electrode. The authors attributed these results to the restriction of the so-called “shuttle effect” favored by the high Li⁺ conductivity of Li₃N that promotes the transformation of insulating Li₂S/Li₂S₂ aggregated on the Li surface to soluble Li₂S_x during the charge process. This was confirmed by SEM analyses that revealed an uneven 100-μm layer of Li₂S/Li₂S₂ on the bare lithium surface after 100 charge/discharge cycles. On the contrary, only 10 μm of this layer was observed for the Li₃N-protected Li.

A LiAl alloy layer was spontaneously created by direct contact between a thin Al foil and lithium metal (Kim et al., 2013). They were pressed together for 24 h under different temperatures to form a highly Li⁺ conducting layer on the Li metal surface. The LiAl-coated lithium presented a rough and cracked surface due to the large volume expansion in Al foil upon alloying. Full cells were assembled with carbide-derived carbon/sulfur composite cathode (CDC/S). Long-term cycling experiments at a C/5 rate showed a capacity retention of only 50% for the cell made with the pristine lithium electrode after 200 cycles. In comparison, the LiAl-protected lithium showed a better capacity retention of 70% and a discharge capacity of 700 mAh g⁻¹ obtained at the end of

testing. Although this LiAl alloy layer seems suitable to lessen the reduction of polysulfides at the lithium surface, the improvement of electrochemical results would be more important if the layer was flatter and more homogeneous.

One of the easiest methods for the surface pre-treatment of lithium is undoubtedly its passivation in liquid media. Liang et al. (2017) recently reported an efficient approach to prevent Li dendrite formation by *in situ* deposition of metallic alloys like Li₁₃In₃, LiZn, Li₃Bi, or Li₃As. The reaction consisted of the reduction of metal chlorides in THF solution by Li (xLi + MCl_x → M + xLiCl with M = In, Zn, Bi, and As) followed by the corresponding alloy formation (yLi + zM → Li_yM_z). XRD, SEM, and XPS analyses confirmed the nature of different alloy layers (~10 μm of thickness), which are covered by resistive LiCl-rich phases preventing the Li⁺ reduction on the surface. Li stripping/plating experiments were monitored in a sealed transparent cell with an optical microscope equipped with a digital camera to follow the growth of dendrite and mossy lithium upon cycling. Before cycling, the surfaces of both unmodified and alloy-modified lithium electrodes were smooth. After 100 cycles (4 mA cm⁻², 10 min) an inhomogeneous deposition of lithium was already observable on fresh lithium electrodes. High-surface-area dendrites slowly formed during subsequent cycles and were very pronounced after 220 cycles, showing highly porous lithium (see **Figure 4** for corresponding operando optical microscopy images). In contrast, the alloy-protected lithium electrodes maintained a smooth surface after 220 cycles. These modified lithium electrodes easily cycled for thousands of cycles in the Li/Li symmetric cell configuration (2 mA cm⁻²) exhibiting low overvoltage, while the cell with bare lithium electrodes short-circuited after 180 h. Moreover, LTO/Li batteries were cycled at a 5C rate for 1,500 cycles. While the cell with fresh lithium failed after only 600 cycles, Li₁₃In₃, LiZn, Li₃Bi, and Li₃As-modified lithium electrodes led to stable cycling up to 1,500 cycles with a capacity retention of ~84% for Li₁₃In₃-lithium, for example. Another example of interesting Li-In alloy was presented by Choudhury et al. (2017). Slightly different from the previous work, the authors used an indium salt [In(TFSI)₃] rather than indium chloride to generate *in situ* the electroless coating [3 Li + In(TFSI)₃ → 3 LiTFSI + In]. The lithium was modified by dipping in a solution of 12 mM In(TFSI)₃ in EC:DEC (1:1) for 6 h before characterization. The XRD pattern of modified lithium confirmed the presence of a Li-In alloy with a small amount of In metal. XPS analyses performed on aged Li electrodes cycled with a standard electrolyte containing In(TFSI)₃ salt showed the presence of an In metallic peak that indicated that the coating remained intact during expansion/contraction of the lithium during cycling. Additionally, the absence of a LiF peak in the F1s spectrum confirmed the ability of the indium layer to prevent side reactions with the electrolyte (namely, decomposition of PF₆⁻). Unfortunately, the authors did not show the results for symmetric or full cells with the pre-treated lithium electrode but preferred to use pristine lithium with an electrolyte containing In(TFSI)₃. Additives in electrolytes are not the scope of the present review; however, since they show the possibility of forming the Li-In alloy before cycling, we will present the most interesting electrochemical results. Long-cycling experiments of



In-Li anodes combined with high-loading commercial cathodes (LTO and NCM) were performed. Almost 90% of the initial discharge capacity was obtained for both the batteries after 250 cycles at a 1C rate.

Another solution-based process for the preparation of an artificial LiF layer on the Li metal surface by a fast precipitation reaction between 1-butyl-2,3-dimethylimidazolium tetrafluoroborate (BdmimBF_4) and Li was proposed by Wang et al. (2019). SEM analysis showed a homogeneous LiF coating with a thickness of $\sim 100 \text{ nm}$, while XPS analysis demonstrated that Li_2O and LiOH generally present on the Li surface were consumed during fluorination. Li plating/stripping experiments in symmetric cells at a high current density of 5 mA cm^{-2} showed poor cycling ability for the cell assembled with pristine lithium since a sudden drop in voltage (dendrites penetrate through the separator) after 32 h (80 cycles) was observed. Stable cycling was obtained for LiF-coated lithium over 240 cycles with an overpotential of $\pm 80 \text{ mV}$. $\text{LiNi}_{0.6}\text{Co}_{0.2}\text{Mn}_{0.2}\text{O}_2/\text{Li}$ batteries were cycled at a 1C rate and the discharge capacity

for the cell assembled with bare lithium dropped sharply to 61.7% of the initial capacity after 100 cycles. By contrast, the cell with LiF-coated lithium maintained a reversible discharge capacity of 144.2 mAh g^{-1} after 100 cycles, corresponding to a capacity retention of 86.5% and presented an average Coulombic efficiency of 99.2% (98% for bare Li).

A Li_3PO_4 layer was created by simple dipping of lithium foil in a DMSO solution containing a small quantity of polyphosphoric acid (Li et al., 2016). After 2 min of reaction, a Li_3PO_4 coating of $\sim 50 \text{ nm}$ thickness was obtained. The coverage was very uniform and a Young's modulus of $\sim 10\text{--}11 \text{ GPa}$ was measured by atomic force microscopy, which is much higher than the 6 GPa needed to suppress Li dendrite formation. This was confirmed by SEM analysis of aged electrodes that still showed smooth surfaces with no porous domains or dendrites (visible for the pristine lithium electrode). This enhancement was also attributed to the high Li^+ conductivity of Li_3PO_4 . LFP/Li batteries were allowed to cycle 200 times at a C/2 rate and after activation of the LFP material. Polarization voltages (difference between charge and

discharge plateau voltages) of 66 and 147 mV were recorded for the cells fabricated with protected and bare lithium, respectively. The reduced resistance was attributed to the better kinetics of the full cell induced by the artificial Li_3PO_4 SEI layer. Finally, after 200 cycles, discharge capacities of 145 and 127 mAh g^{-1} were obtained for cells assembled with Li_3PO_4 -modified and pristine lithium electrodes, respectively. A dual-layered film was constructed on the Li metal anode by direct immersion of lithium in the well-known fluoroethylene carbonate (FEC) solvent (Yan et al., 2018).

The reduction in FEC yielded a rigid inorganic-rich layer (Li_2CO_3 and LiF) of ~ 50 nm on the bottom accompanied by a compact organic layer (ROCO₂Li and ROLi) of 25 nm thickness on the top. The Young's modulus of the top layer was around 0.6 GPa while that of the underlying inorganic layer was ~ 7.0 GPa, high enough to suppress dendrite growth. Furthermore, SEM analyses of aged bare lithium electrodes from symmetrical Li/Li cells showed porous and loose structures after only 10 cycles at 2.5 mA cm^{-2} . In comparison, the surface of the protected Li maintained a smooth flat morphology, without the formation of dendritic or dead lithium. The electrolyte decomposition was also highly reduced after lithium modification since the R_{CT} increased from 40 to 49 Ω for modified lithium and from 69 to 94 Ω for bare lithium between the first and the 50th cycle. Both protected and pristine Li anodes were paired with NCM cathodes and cycled at a C/2 rate. Protected Li exhibited a superior capacity retention of 68.2% compared with the 19.1% of pristine Li after 120 cycles. In addition, the average Coulombic efficiency for the cell made with protected and pristine Li reached 99.5 and 98.1%, respectively.

A protective layer, mainly composed of LiI and LiO_3 ionic conductive materials, was deposited on the lithium surface by immersing it in a DMSO solution containing HIO_3 acid (Jia et al., 2017). After chemical treatment, the lithium foil displayed a smooth and tight surface, and the chemical composition of the layer was confirmed by XPS analyses. Li/Li symmetric cells were assembled and the evolution of R_{CT} was followed in time. Its value increased from 280 to 650 Ω (pristine lithium) and from 230 to 397 Ω (modified lithium) after 2 and 48 h of standing time, respectively. A symmetrical cell assembled with HIO_3 -treated lithium was able to cycle under a constant current of 0.5 mA cm^{-2} for more than 400 h while the cell with bare lithium electrodes exhibited higher overvoltage (70 mV against 30 mV after modification) and short-circuited after ~ 210 h. The average Coulombic efficiency after 50 cycles for the Li/Cu cell made with coated Li was near 91% whereas 82% was obtained with bare lithium foil, which was completely destroyed after 60 cycles. Electrochemical performances of Li/S batteries were also improved with the surface treatment since after long-term cycling experiments of 500 cycles at a C/2 rate, average Coulombic efficiencies of 93 and 88% and discharge capacities of 506 and 401 mAh g^{-1} were obtained for cells made with protected and bare lithium, respectively. These improved performances originated from the ion-conductive film induced by HIO_3 treatment that promotes homogeneous deposition of lithium on the anode side and reduces direct contact between the electrolyte and the Li surface.

The effect of salt addition (LiFSI , LiPF_6 , and LiAsF_6) in $[\text{C}_3\text{mPyr}^+][\text{FSI}^-]$ ionic liquid to be further used as dipping solutions for lithium modification was presented by O'Mullane's research group (Basile et al., 2016). A major part of this study was dedicated to understanding the mechanism for the formation of the SEI depending on parameters such as time of immersion and salt used. It was found that the major constituents of the mineral SEI formed after pre-treatment are LiF, Li_2CO_3 , LiSO_2F , and LiOH as well as cation breakdown products via a Hofmann elimination mechanism. Long-duration reactions (10–12 days but < 18 days) were needed to yield a robust SEI layer. Symmetric cells assembled with different modified lithium electrodes showed particularly good stability over 200 cycles. More interestingly, Li/LFP cells were assembled and allowed to cycle at a 1C rate for 1,000 cycles. The pristine lithium cell displayed an average Coulombic efficiency of 99.6%; however, the CE plot underwent fluctuations and became unstable after ~ 600 cycles where efficiency dropped to 95.75%. After a long period of instability, a capacity retention of 80% was obtained, also after 600 cycles. In comparison, the final CE values after 1,000 cycles for the $\text{LiPF}_6/[\text{C}_3\text{mPyr}^+][\text{FSI}^-]$ - and $\text{LiAsF}_6/[\text{C}_3\text{mPyr}^+][\text{FSI}^-]$ -pre-treated cells were 99.02 and 99.89%, respectively. High capacity retentions of 95.2 and 95% were calculated for these two modified cells.

Chemical Reaction With Silanes

Silane and especially chlorosilane molecules are adapted for the surface modification of lithium since they easily react with OH groups present on the native film to yield strong Si-O and Li-Cl bonds generally observed by XPS or FTIR analyses after treatment. Since several examples of functionalization of Li metal by silane were reported in the literature, we chose to present these results in a separate section.

The influence of substituent size of chlorosilane molecules (R-Cl with R = Me_3Si -, MeSiCl_2 -, MePropSiCl -, MePhSiCl -, Et_3Si -, $i\text{-Prop}_3\text{Si}$ -, Ph_3Si -, or $t\text{-Bu}_3\text{Si}$ -) on cycle life of LTO/Li cells created with different treated lithium foils was compared (Neuhold et al., 2012). First, authors showed that razor-cleaned and pentane-washed lithium led to lower interfacial resistance due to the removal of resistant native film. Thus, this cleaned lithium was selected to be modified by dipping in the different chlorosilane solutions. The number of cycles required to reduce the LTO/Li cells capacities to 80 and 60% of their original values was compared to the calculated R-group size of silanes used for the modifications. In rapid conclusion, very small R-groups (Me_3Si - with $V = 98.7 \text{ \AA}^3$) and R-groups bulkier than triphenyl (Ph_3Si - with $V = 263.2 \text{ \AA}^3$) showed enhanced cycle life compared to the bare lithium. For instance, the cell assembled with Me_3Si -modified lithium reached 60% of its initial discharge capacity after 209 cycles while only 80 cycles were necessary for the cell made with bare lithium. Inversely, intermediately sized R-groups showed reduced cycle life. With small R groups, good coverage of the lithium surface was possible, which reduces contact with electrolyte and side reactions. For large R groups, fewer surface links are possible but the steric hindrance induced by these groups also impedes electrolyte molecules reaching the Li surface. The same research group specifically studied the

effect of trimethylsilyl- (TMS-) and triisopropylsilyl-modified (TIPS-) lithium electrodes on the electrochemical performance of LTO/Li batteries (Thompson et al., 2011). The modified lithium foils were characterized by FTIR and the smaller TMS group was found to have a more intense FTIR peak at $1,050\text{ cm}^{-1}$ than for TIPS-modified Li, indicating more Si-O bonds and thus higher surface coverage. A simple surface-packing hard sphere model was used to demonstrate that two times more TMS groups could be attached to the surface in comparison to TIPS moieties. As concluded above, better uniformity of silane coverage led to better electrochemical performance. In fact, after 100 charge/discharge cycles at a current density of 1 mA cm^{-2} , the cells assembled with the bare, TIPS-modified, and TMS-modified lithium electrodes showed capacity retentions of ~ 40 , 60 , and 80% , respectively. Marchioni et al. (2007) also reported a study dealing with the size effect of R-substituent of chlorosilanes on the electrochemical performance of Ni/Li cells. The FTIR spectrum for chlorotrimethylsilane-treated lithium metal showed disappearance of the LiOH band at $3,677\text{ cm}^{-1}$, which is generally observed for pristine lithium. Its absence confirmed the reaction between the native layer on Li metal surface and the chlorosilane, yielding a LiCl (detected by XPS analysis) by-product and H_2 gas. Additionally, the Si-O bond at $\sim 1,050\text{ cm}^{-1}$ was clearly visible. The influence of the chain length on the evolution of the charge-transfer resistance of modified lithium electrodes was followed as a function of electrolyte immersion time. It was concluded that lithium modified with silane containing short alkyl chains gave the smaller R_{CT} resistances, even after 7 days of immersion. By contrast, silanes containing alkyl chains longer than ethyl [namely, chloro(dodecyl)dimethylsilane] exhibited a gradual increase in impedance with immersion time, and was higher than that of pristine lithium after 7 days. This detrimental result was due to the steric effect of long chains that limits the formation of dense coverage.

Neuhold et al. (2014) reported the modification of lithium with cyclopentadienyldicarbonyl iron (II) silanes (Fp-silanes). The proposed mechanism involves breaking the Fe-Si bond with the Fp moiety acting as a leaving group and resulting in a SiR_3 -terminated surface bonded through the surface oxygen group. The effect of several coating agents (FpSiPh₃, FpSiMe₃, and FpSiMe₂H) on the cyclability of LTO/Li cells was studied. It was found that, after modification, the cycle life of the batteries increased, although lower initial discharge capacities were obtained due to the increase in interfacial resistance. For instance, the cycle life performance increased from ~ 60 cycles, for bare lithium, to more than 300 cycles for the FpSiMe₂H-modified lithium electrode. Inversely, the average capacity over 60 cycles for pristine lithium was around 0.63 mAh cm^{-2} when a quite stable 0.26 mAh cm^{-2} was obtained for FpSiMe₂H-modified lithium over 300 cycles. The effect of immersion time in FpSiPh₃ silane solution was also studied and the best compromise was obtained for lithium electrodes dip-coated for only 10 min to avoid an overly thick layer leading to poor electrochemical results.

The same authors recently published a study based on the reactivity of lithium with vinyl-substituted silanes

[trivinylchlorosilane (TVCS) and divinylchlorosilane (DVDCS)] (Buonaiuto et al., 2015). Their strategy was to create a two-dimensional coating attached to the surface by electro-polymerization of vinyl substituents that is known to happen around 0.8 V . Hence, during the first charge of a LTO/Li battery, a self-induced polymer network on top of the lithium was created. This was confirmed by FTIR spectra of TVCS- and DVDCS-modified Li electrodes after one cycle that showed the absence of a peak at $1,595\text{ cm}^{-1}$ attributed to the vinyl groups. However, the electrochemical results were not greatly improved after modifications and a rapid capacity fading was observed for all LTO/Li cells. For instance, after 120 cycles (1.5 mA cm^{-2}), the cells assembled with pristine and DVDCS-modified Li electrodes retained ~ 38 and 25% of their initial capacity, respectively. This slight enhancement in stability was attributed to the self-formed polymer layer that partially reduces the contact between electrolyte and lithium. However, SEM analyses of the polymer layer and post-mortem results are needed to support this hypothesis but are absent in this study.

Slightly different from the aforementioned examples of Li-surface modification by chlorosilane, Wu et al. (2016) proposed the ingenious pre-treatment of lithium with oxygen atmosphere before modification with trimethylsilyl chloride. This method permits the increase of the thickness of the hydroxyl-containing layer, which led to thicker coating with better homogeneity after reaction with silane (84 nm thick in this example). The reaction was confirmed by XPS analysis that revealed a broad Si 2p peak at $\sim 101.4\text{ eV}$ corresponding to Si-O and Si-C bonds. The variation in the AC impedance spectra as a function of the storage time in Li/Li symmetric cells was followed. The value of R_{SEI} (related to the high-frequency semi-circle corresponding to the SEI layer) for the cell made with modified lithium electrodes ($\sim 50\ \Omega$) was two times less than that assembled with bare lithium ($\sim 100\ \Omega$), which fluctuated extensively with time. This result showed that the SEI film formed on modified Li electrode surface was more conductive and effectively restricted the access of electrolyte to the Li surface. The Li/S battery with a modified Li anode exhibited better cycling performance, since after 100 cycles at a C/2 rate, a discharge capacity of 760 mAh g^{-1} was obtained that corresponds to a capacity retention of 71% . In contrast, a capacity retention of only 40% (417 mAh g^{-1}) was obtained with the pristine lithium anode. The modification of lithium can be also achieved using silicon alkoxide rather than chlorosilane.

An example of surface functionalization employing tetraethoxysilane (TEOS) as reactive species was recently reported (Umeda et al., 2011). An $\sim 1\text{-}\mu\text{m}$ -thick artificial SEI layer was obtained after soaking lithium in pure TEOS for 5 min. The effect of this layer on the evolution of charge-transfer resistance was first evaluated in a Li/Li symmetric cell at OCV state. Interestingly, with TEOS-modified lithium, the R_{CT} value remained quite stable around $40\ \Omega$ during 20 days of storage while that for pristine lithium increased from 230 to $330\ \Omega$ between the 1st and the 20th cycle. Plating/stripping experiments performed at 1 mA cm^{-2} showed invariance in R_{CT} ($\sim 34\ \Omega$) for the cell made with modified lithium electrodes even after 20 cycles. Compared with bare lithium, the R_{CT} slowly decreased during cycling but remained higher than for the modified-Li

cell after 10 cycles (197 Ω). These results, supported by SEM observation of aged electrodes, demonstrated the protective role of the TEOS-grafted layer against electrolyte degradation and also avoided the formation of high area lithium. A hybrid silicate coating was performed on O₂-pre-treated lithium by exposing it to the mixed vapors of 3-mercaptopropyl trimethoxysilane (MPS) and TEOS (1:1 precursor volume ratio) at 100°C for 8 h (Liu et al., 2018). According to the authors, the resulting thin (~24 nm thick) compact organic-inorganic coating possesses a “hard” inorganic moiety (Li_xSiO_y) to block the growth of Li dendrites and a “soft” organic moiety (mercaptopropyl groups) to enhance the flexibility, robustness, and the artificial SEI layer. This grafting mechanism was validated by FTIR and XPS analyses that notably showed a peak at 101.6 eV on the Si 2p spectrum that is characteristic of the formation of lithium silicate (Li_xSiO_y). Moreover, on the S 2p spectrum, a peak at 161.3 eV confirmed the presence of -S-Li bonds. The electrochemical performance of a Li/Li symmetric cell made with hybrid silicate-modified lithium was greatly improved since stable charge/discharge plateaus with an overvoltage of ± 45 mV were obtained during 125 stripping/plating cycles at 0.5 mA cm⁻². By contrast, after only 13 cycles, the cell with uncoated lithium showed a rapid increase in overpotential with important fluctuations. Li/LFP batteries were also assembled and cycled at a rate of C/2 with a conventional carbonate-based electrolyte. After 500 cycles, the cell with a coated-Li anode exhibited a reversible capacity of 103.6 mAh g⁻¹ (CR = 75%) and an average Coulombic efficiency of 99.87%, while the cell with bare lithium suffered from rapid deterioration after 200 cycles.

Finally, our research group recently presented the modification of lithium with cross-linkable silane groups before covering with a 4- μ m-thick layer of ally-ether ramified polyethylene oxide polymer (PEO) (Delaporte et al., 2019). The aim of this double modification was to first create a passivation layer on the lithium surface to avoid side reactions with the electrolyte and second to make the lithium stickier to facilitate combination with LLZO garnet solid electrolyte. After the cross-linking reaction under UV light, a strong link between the lithium, the organosilane, and the polymer layers was obtained. The AC impedance spectrum of the Li/Li symmetric cell made with LLZO electrolyte and pristine lithium electrodes showed an overall resistance of ~550 k Ω at 25°C. After deposition on lithium of only a layer of polymer, this resistance decreased to ~40 k Ω and reached 12 k Ω when the silane and the polymer layers were both deposited. Li stripping/plating experiments at 80°C confirmed the improved contact between garnet and lithium and the better passivation of lithium by the silane layer. Additionally, the cell made with pristine lithium showed higher overvoltage for each cycling current and short-circuited after <130 h of cycling under a constant current of 0.05 mA cm⁻². In contrast, the cells made with polymer-coated and silane/polymer-coated lithium electrodes showed smaller voltage hysteresis of ~80 and 50 mV under a constant current of 0.1 mA cm⁻². Moreover, during cycling, the charge/discharge plateaus were completely flat for the cell with silane/polymer-coated lithium, presuming an excellent electrodeposition of lithium

under the silane layer, which was not observed when only a polymer layer was deposited. In the future, after careful removal of the polymer layer, we will perform post-mortem SEM investigations on aged lithium to confirm our hypothesis and support electrochemical results.

Mechanical Modification

Non-uniform current density originating from any surface defects or solid electrolyte interphases (SEI) will inevitably result in the formation of high surface area lithium (HSAL) with a mossy, granular, or dendritic morphology. The formation of HSAL can be easily reduced employing low currents for Li plating; however, this criterion is rarely respected in most batteries due to power-demanding applications. To fix this issue, attempts have been made to increase the active surface area of Li metal and thus to decrease the actual current density of the Li metal battery.

With this aim, a micro-needle surface treatment technique for Li metal foil was proposed by Bieker's research group (Ryou et al., 2015). They used a micro-needle roller (generally found in cosmetics shops) with 340 arrays with a length of 200 μ m to decorate the lithium with holes distributed evenly on its surface. The Li/Li symmetrical cell employing bare lithium showed a higher overall resistance after one cycle at a C/10 rate than the cell assembled with hole-decorated-lithium. This was attributed to the fact that the surface area of the treated Li metal was much larger than that of bare Li metal while the electrodes have the same geometric dimension. LFP/Li cells assembled with both treated and pristine lithium anodes were run for 150 cycles at a C/2 rate. A discharge capacity of ~1.0 mAh was obtained at the end of the experiment for the modified cell, which corresponded to a capacity retention of 85%. In comparison, the pristine cell presented a poor retention capacity of only 26% (0.3 mAh) and was characterized by a sudden loss of capacity after 70 cycles. To understand the reason for this enhancement, the authors investigated the morphological structural changes in the “hole-wall surfaces.” They observed that after cycling, the original vertical striation pattern of the hole wall became embossed, which implies that Li deposited alongside these unique wall structures in the hole. In other words, until the holes are fully filled with Li, no plating on the flat surface will take place and thus HSAL formation is delayed. **Figure 5** presents SEM images of cycled lithium electrodes, which showed an augmentation of granular-type lithium in the holes when the cycling current was increased. One year later, the same authors presented a deeper study on the subject by proposing the Li surface modification with a stainless steel stamp with micrometer-scale pyramidal reliefs (height = 50 μ m, width = 50 μ m, ridge length = 40 μ m) (Park et al., 2016). Before choosing these specific dimensions, they simulated the current density profile on the Li metal surface with different surface patterns with COMSOL Multiphysics software. The resulting modeling assumed that the current density inside the holes formed by the inverted pyramids was greater (0.56 mA cm⁻²) than on the flat lithium surface (0.44 mA cm⁻²), and by consequence, during Li plating and stripping processes, Li ions should reversibly fill and drain surface pattern holes. This is exactly what they observed by SEM analyses after cycling.

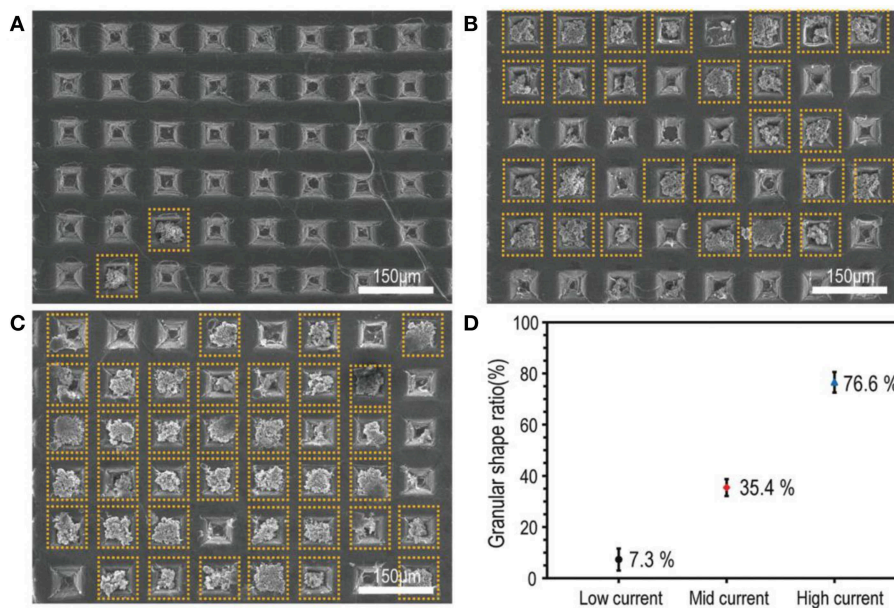


FIGURE 5 | SEM images of cycled lithium electrodes with a constant current of (A) $+0.15 \text{ mA cm}^{-2}$ (low current) for 80 min, (B) $+0.6 \text{ mA cm}^{-2}$ (mid current) for 20 min, and (C) $+2.4 \text{ mA cm}^{-2}$ (high current) for 5 min. Granular-type lithium is indicated with dashed-line squares. (D) The probability of granular features on the surface patterned Li metal as a function of current density. Reprinted with permission from Park et al. (2016). Copyright (2016) John Wiley and Sons.

The holes were effectively filled with granular-shaped lithium during the plating step and after stripping all the lithium was removed. Even after 100 cycles of charge/discharge, the surface-patterned lithium maintained its original morphological structure. Consequently, better performances in Li/Li symmetric cells were reported and the cycling life of $\text{LiMn}_2\text{O}_4/\text{Li}$ batteries was also greatly increased. In fact, after 450 cycles at a $C/2$ rate, the cell constructed with surface-patterned lithium delivered a discharge capacity of 88.9 mAh g^{-1} , corresponding to a capacity retention of 88.7%, which is higher in comparison to the poor 43.9% (42.7 mAh g^{-1}) obtained for pristine lithium after only 250 cycles.

Becking et al. (2017) reported the effect of roll-pressing the lithium foil on the electrochemical performance of a lithium-metal anode. The surface of the as-received lithium was characterized by AFM, which revealed an average roughness of $\sim 130 \pm 10 \text{ nm}$ at its surface. These mountain-like structures with deep valleys can act as preferential “hot spots” for Li^+ dissolution and deposition. After roll-pressing, the surface was smoother with fewer mountain-like structures and the roughness decreased to $\sim 37.3 \text{ nm}$. Li/Li symmetrical cells were cycled for 50 cycles (0.1 mA cm^{-2}) and the evolution of R_{SEI} was followed. Interestingly, during the first 10 cycles, the resistance was lower for the roll-pressed lithium-metal anode but rejoined that of pristine lithium during the following 40 cycles. The authors concluded that the roll-press technique reduced the thickness of the native surface film, which led to lower impedance in the first cycles. This was confirmed with the charge/discharge profiles of the stripping/plating experiment that showed a higher overvoltage ($+85 \text{ mV}$ and -48 mV) on the first cycle for

pristine lithium than for the roll-pressed lithium ($+17 \text{ mV}$ and -17 mV). However, with cycling, both cells presented stable and similar charge/discharge plateaus with overvoltages of $\pm 20 \text{ mV}$. Finally, SEM images of aged electrodes showed homogeneous HSAL deposition for the roll-pressed lithium foil after a few cycles, and the morphology for both the electrodes was similar after 15 cycles.

SEI Formation Before Reassembling

This last section reports some examples of artificial SEI layers pre-formed on lithium surface by electrochemistry directly in the battery. After disassembling the cell, the Li-metal anode with the implantable SEI can be paired with the desired cathode. Although these examples respect the scope of this review, their scale-up remains improbable and challenging.

The electroreduction at a Li-metal electrode of FEC additive in electrolyte was recently reported to create an artificial LiF-rich layer also composed of Li_2CO_3 , polyene and C-F bond-containing compounds (Liu et al., 2015). After film forming, the symmetric cell was disassembled and the FEC-modified lithium anode (covered with a layer of dark film) was employed in Li/ O_2 batteries. Impedance spectra of the Li/ O_2 cell assembled with pristine lithium showed an increase in charge-transfer resistance from 160 to 440Ω after 60 h at OCV. In contrast, no significant impedance change (from 140 to 150Ω) was observed when an FEC-modified lithium anode was employed, confirming the role of the artificial SEI against corrosion induced by electrolyte or dissolved O_2 . By limiting the cell capacity to $1,000 \text{ mAh g}^{-1}$, long-cycling experiments at a constant charge/discharge current of 300 mA g^{-1} were achieved. While the cell with pristine lithium

TABLE 1 | Compilation of different types of pre-treatments on lithium metal foil and their effects on the improvement of electrochemical performance.

Type of modification	Nature of modification	Best electrochemical improvement observed	References
Polymer coating	20-nm-thick PAA layer	W modification: Li/NMC111 battery: 2.8 mAh cm ⁻² , 1 mA g ⁻¹ , 40 cycles, CR = 82.3%, CE = 96.5% W/O modification: Li/NMC111 battery: 1.0 mAh cm ⁻² , 1 mA g ⁻¹ , 40 cycles, CR = 29.4%, CE = 92.5%	Li et al., 2018
	150-nm-thick P(VC-co-AN) layer	W modification: LCO/Li battery: 126 mAh g ⁻¹ , C/2, 100 cycles, CR = 91% W/O modification: LCO/Li battery: 102 mAh g ⁻¹ , C/2, 100 cycles, CR = 76%	Choi et al., 2013
	10-μm-thick poly(ethylene glycol) dimethacrylate layer	Suppression of reaction between polysulfides and Li anode Stable discharge capacity of 270 mAh g ⁻¹ for up to 100 cycles for a Li-S battery	Lee et al., 2003
	10-μm-thick layer of PEDOT-co-PEG polymer	W modification: Li/S battery: 876 mAh g ⁻¹ , C/5, 200 cycles, CE = 89% W/O modification: Li/S battery: 400 mAh g ⁻¹ , C/5, 200 cycles, CE = 81%	Ma et al., 2014a
	380-nm-thick layer of PEDOT-co-PEG polymer	W modification: LCO/Li battery: 118 mAh g ⁻¹ , C/2, 200 cycles, CR = 87.3% W/O modification: LCO/Li battery: 13 mAh g ⁻¹ , C/2, 200 cycles, CR = 9.3%	Kang et al., 2014
	Polyacetylene film (PA)	W modification: LCO/Li battery: R _{el} = 3 Ω, R _{CT} = 40 Ω W/O modification: LCO/Li battery: R _{el} = 25 Ω, R _{CT} = 380 Ω	Belov et al., 2006
	Poly(ethyl α-cyanoacrylate) film + LiNO ₃ salt	W modification: LFP/Li battery: 137 mAh g ⁻¹ , 2C, 500 cycles, CR = 93% W/O modification: LFP/Li battery: 25 mAh g ⁻¹ , 2C, 500 cycles, CR = 5%	Hu et al., 2017
	3.5-μm-thick layer of 1,6-hexanediol diacrylate polymerized with Kynar 2801	W modification: LCO/Li battery: 108 mAh g ⁻¹ , C/2, 100 cycles, CR = 80% W/O modification: LCO/Li battery: 25 mAh g ⁻¹ , C/2, 40 cycles, CR = 20%	Choi et al., 2004a
	3.5-μm-thick layer of 1,6-hexanediol diacrylate polymerized with Kynar 2801 + OEGB	W modification: LCO/Li battery: 115 mAh g ⁻¹ , C/2, 100 cycles, CR = 85% W/O modification: LCO/Li battery: 25 mAh g ⁻¹ , C/2, 40 cycles, CR = 20%	Choi et al., 2004b
	Polymer coating containing ceramics	SBR film + nanometric Cu ₃ N particles	W modification: Cu/Li battery: 1 mAh cm ⁻² , 100 cycles, CE = 97.4%. LTO/Li battery: 135 mAh g ⁻¹ , C/2, 90 cycles, CE = 97.4% W/O modification: Cu/Li battery: 1 mAh cm ⁻² , 50 cycles, CE = 70%. LTO/Li battery: 125 mAh g ⁻¹ , C/2, 20 cycles, CE = 88.3%
20-μm-thick layer of PVDF-HFP with Al ₂ O ₃ particles		W modification: Co ₃ O ₄ -Super P/Li battery: stable 1,000 mAh g _{carbon} ⁻¹ , 0.1 mA cm ⁻² , 80 cycles W/O modification: Co ₃ O ₄ -Super P/Li battery: 320 mAh g _{carbon} ⁻¹ , 0.1 mA cm ⁻² , 80 cycles	Lee et al., 2014
1.7- to 3.7-μm-thick layer of PVDF with Al ₂ O ₃ particles		W modification: Li/S battery: 850 mAh g ⁻¹ , 160 mA g ⁻¹ , 50 cycles, CR = 70% W/O modification: Li/S battery: 550 mAh g ⁻¹ , 160 mA g ⁻¹ , 50 cycles, CR = 50%	Jing et al., 2015
Polyimide film + nanometric Al ₂ O ₃ particles		W modification: Li/Li battery: R _{CT} = 120 Ω cm ⁻² , 8 h cycling. LFP/Cu battery: 111.6 mAh g ⁻¹ , C/5, 20 cycles, CE = 97.5% W/O modification: Li/Li battery: R _{CT} = 18 Ω cm ⁻² , 160 h cycling. LFP/Cu battery: 4.1 mAh g ⁻¹ , C/5, 3 cycles, CE = not mentioned	Peng et al., 2016
Carbon coating		r-GO layer	W modification: LFP/Li battery: 128.8 mAh g ⁻¹ , 1C, 300 cycles, CR = 99% W/O modification: LFP/Li battery: 89.5 mAh g ⁻¹ , 1C, 300 cycles, CR = 69%
	FG layer	W modification: LFP/Li battery: 94.4 mAh g ⁻¹ , 1C, 250 cycles, CR = 81%. Li/S battery: 440 mAh g ⁻¹ , C/5, 100 cycles, CE = 53% W/O modification: results not shown	Bobnar et al., 2018
	GO layer	W modification: Li/S battery: 707 mAh g ⁻¹ , C/10, 200 cycles, CR = 69% W/O modification: Li/S battery: 487 mAh g ⁻¹ , C/10, 200 cycles, CR = 58%	Zhang et al., 2016a
	GO self-standing film	W modification: Cu/Li battery: 100 cycles, CE = 90% W/O modification: Cu/Li battery: 40 cycles, CE = 70%; short-circuited after 50 cycles	Zhang et al., 2016b
	MWCNT self-standing film	W modification: Li/SC battery: 854 mAh g ⁻¹ , C/2.5, 70 cycles, CR = 97% W/O modification: Li/SC battery: Capacity not found, C/2.5, 70 cycles, CR = 90%	Salvatierra et al., 2018
	Carbon coating by sputtering method	Amorphous carbon film	W modification: Cu/Li battery: 0.25 mAh cm ⁻² , 50 cycles, CE = 80% W/O modification: Cu/Li battery: 0.25 mAh cm ⁻² , 50 cycles, CE = 40%

(Continued)

TABLE 1 | Continued

Type of modification	Nature of modification	Best electrochemical improvement observed	References
Inorganic coating by sputtering method	10-nm-thick MoS ₂ layer	W modification: Li/S battery: 1,200 mAh g ⁻¹ , C/10, 300 cycles, CR = 67%; 940 mAh g ⁻¹ , C/2, 1,200 cycles, CR = 84% W/O modification: Li/S battery: 1,000 mAh g ⁻¹ , C/10, 150 cycles, CR = 55%	Cha et al., 2018
	30-nm-thick Li ₃ PO ₄ layer	W modification: Li/S battery: 486 mAh g ⁻¹ , C/2, 200 cycles, CR = 52%, CE = 89% W/O modification: Li/S battery: 247 mAh g ⁻¹ , C/2, 200 cycles, CR = 28%, CE = 84%	Wang et al., 2017
	950-nm-thick LiPON layer	W modification: Li/Li battery: R _{CT} = 500 Ω cm ⁻² , 50 cycles, 10 mA cm ⁻² W/O modification: Li/Li battery: R _{CT} = 1,750 Ω cm ⁻² , 50 cycles, 10 mA cm ⁻²	Chung et al., 2004
	330-nm-thick Li _x Si layer	W modification: LFP/Li battery: 136 mAh g ⁻¹ , 2C, 350 cycles, CR = >99% W/O modification: LFP/Li battery: 60 mAh g ⁻¹ , 2C, 350 cycles, CR = 50%	Tang et al., 2018
	20-nm-thick Al ₂ O ₃ layer	W modification: Li/Li battery: R _{overall} = 365 Ω, 100 cycles, 0.1 mA cm ⁻² , polymer electrolyte, 50°C W/O modification: Li/Li battery: R _{overall} = 442 Ω, 100 cycles, 0.1 mA cm ⁻² , polymer electrolyte, 50°C	Wang et al., 2018
	150-nm-thick LiF layer	W modification: Li/Cu battery: 1 mAh cm ⁻² , 90 cycles, CE = 99% W/O modification: Li/Cu battery: 1 mAh cm ⁻² , 90 cycles, CE = 60%	Fan et al., 2017
Inorganic coating by ALD	2- to 4-nm-thick Al ₂ O ₃ layer	W modification: Li/Li battery: Stable for 1,100 cycles, 1 mA cm ⁻² . After 250 cycles, R _{CT} = 50 Ω W/O modification: Li/Li battery: Stable for 600 cycles, 1 mA cm ⁻² . After 250 cycles, R _{CT} = 140 Ω	Kazyak et al., 2015
	14-nm-thick Al ₂ O ₃ layer	W modification: Li/S battery: 1,080 mAh g ⁻¹ , 100 cycles, CR = 90%. 1st cycle, CE = 95% W/O modification: Li/S battery: 600 mAh g ⁻¹ , 100 cycles, CR = 50%. 1st cycle, CE = 70%	Kozen et al., 2015
Gas reaction	40-nm-thick LiF layer	W modification: Li/S battery: 1,050 mAh g ⁻¹ , C/2, 100 cycles, CR = 91%, CE = 99% W/O modification: Li/S battery: 750 mAh g ⁻¹ , C/2, 100 cycles, CR = 73%, CE = 99%	Lin et al., 2017b
	380-nm-thick LiF layer	W modification: Li/S battery: 1,050 mAh g ⁻¹ , C/5, 100 cycles, CR = 95%, CE = 99% W/O modification: Li/S battery: 900 mAh g ⁻¹ , C/5, 100 cycles, CR = 82%, CE = 95.7%	Zhao et al., 2017
	160-nm-thick Li ₃ N layer	W modification: Cu/Li battery: 0.25 mAh cm ⁻² , 100 cycles, CE = 89% W/O modification: Cu/Li battery: 0.25 mAh cm ⁻² , 100 cycles, CE = 70%	Wu et al., 2011
	200- to 300-nm-thick Li ₃ N layer	W modification: Li/S battery: R _{CT} = 92 Ω, 240 h cycling. 956.6 mAh g ⁻¹ , C/5, 200 cycles, CE = 79.7% W/O modification: Li/S battery: R _{CT} = 168 Ω, 240 h cycling. 452.2 mAh g ⁻¹ , C/5, 200 cycles, CE = 37.2%	Ma et al., 2014b
Metal-to-metal reaction	LiAl alloy layer	W modification: Li/CDC/S battery: 700 mAh g ⁻¹ , C/5, 200 cycles, CR = 70% W/O modification: Li/CDC/S battery: 550 mAh g ⁻¹ , C/5, 200 cycles, CR = 50%	Kim et al., 2013
Liquid reaction	10-μm-thick Li ₁₃ In ₃ , LiZn, Li ₃ Bi and Li ₃ As alloys layer	W modification (ex: Li ₁₃ In ₃): LTO/Li battery: 135 mAh g ⁻¹ , 5C, 1,500 cycles, CR = 84% W/O modification: LTO/Li battery: short-circuited, 5C, 600 cycles	Liang et al., 2017
	Li-In alloy layer	W modification: Li/NMC battery: 112 mAh g ⁻¹ , 1C, 250 cycles, CR = 90%, CE = >98%. Li/LTO battery: 148 mAh g ⁻¹ , 1C, 250 cycles, CR = 90%, CE = >98% W/O modification: results not shown	Choudhury et al., 2017
	100-nm-thick LiF layer	W modification: Li/NMC622 battery: 144.2 mAh g ⁻¹ , 1C, 100 cycles, CR = 86.5%, CE = 99.2% W/O modification: Li/NMC622 battery: 97.7 mAh g ⁻¹ , 1C, 100 cycles, CR = 61.7%, CE = 98%	Wang et al., 2019
	50-nm-thick Li ₃ PO ₄ layer	W modification: LFP/Li battery: 145 mAh g ⁻¹ , C/2, 200 cycles, CR = 97%, ΔE = 66 mV	Li et al., 2016

(Continued)

TABLE 1 | Continued

Type of modification	Nature of modification	Best electrochemical improvement observed	References
		W/O modification: LFP/Li battery: 127 mAh g ⁻¹ , C/2, 200 cycles, CR = 84%, ΔE = 147 mV	
	75-nm-thick dual-layered film	W modification: Li/Li battery: R _{CT} = 49 Ω, 50 cycles, 5 mA cm ⁻² , 0.5 mAh cm ⁻² . NMC/Li battery: 105 mAh g ⁻¹ , C/2, 120 cycles, CR = 68.2%, CE = 99.5%	Yan et al., 2018
	Li/LiO ₃ composite layer	W/O modification: Li/Li battery: R _{CT} = 94 Ω, 50 cycles, 5 mA cm ⁻² , 0.5 mAh cm ⁻² . NMC/Li battery: 26 mAh g ⁻¹ , C/2, 120 cycles, CR = 19.1%, CE = 98.1%	
		W modification: Cu/Li battery: 0.5 mAh cm ⁻² , 50 cycles, CE = 91%. Li/S battery: 506 mAh g ⁻¹ on average, C/2, 500 cycles, CE = 93% on average	Jia et al., 2017
	Multi-minerals layer	W/O modification: Cu/Li battery: 0.5 mAh cm ⁻² , 50 cycles, CE = 82%. Li/S battery: 401 mAh g ⁻¹ on average, C/2, 500 cycles, CE = 88% on average	
		W modification: LFP/Li battery: 63 mAh g ⁻¹ , 1C, 1,000 cycles, CR = 95%, CE = 99.89% (for LiAsF ₆ /[C ₃ mPyr ⁺][FSI ⁻]-pretreated lithium)	Basile et al., 2016
		W/O modification: LFP/Li battery: 60 mAh g ⁻¹ , 1C, 600 cycles, CR = 80%, CE = 95.75%	
Chemical reaction with silanes	Me ₃ Si-modified lithium	W modification: LTO/Li battery: 1.5 mA cm ⁻² , 209 cycles, CR = 60%	Neuhold et al., 2012
		W/O modification: LTO/Li battery: 1.5 mA cm ⁻² , 80 cycles, CR = 60%	
	Me ₃ Si-modified lithium	W modification: LTO/Li battery: 1 mA cm ⁻² , 100 cycles, CR = 80%	Thompson et al., 2011
		W/O modification: LTO/Li battery: 1 mA cm ⁻² , 100 cycles, CR = 40%	
	Me ₃ Si-modified lithium	W modification: Li/Ni battery: R _{CT} = 5.0 Ω cm ⁻² , 7 days in electrolyte	Marchioni et al., 2007
		W/O modification: Li/Ni battery: R _{CT} = 44.3 Ω cm ⁻² , 7 days in electrolyte	
	Me ₂ HSi-modified lithium	W modification: LTO/Li battery: 2.5 mA cm ⁻² , 0.26 mAh cm ⁻² on average, >300 cycles	Neuhold et al., 2014
		W/O modification: LTO/Li battery: 2.5 mA cm ⁻² , 0.63 mAh cm ⁻² on average, 60 cycles	
	(CH ₂ CH ₂) ₂ Cl-modified lithium	W modification: LTO/Li battery: 1.5 mA cm ⁻² , 60 mAh g ⁻¹ , 120 cycles, CR = 38%	Buonaiuto et al., 2015
		W/O modification: LTO/Li battery: 1.5 mA cm ⁻² , 40 mAh g ⁻¹ , 120 cycles, CR = 25%	
	O ₂ -treated and Me ₃ Si-modified lithium	W modification: Li/S battery: 760 mAh g ⁻¹ , C/2, 100 cycles, CR = 71%, CE = 98%	Wu et al., 2016
		W/O modification: Li/S battery: 417 mAh g ⁻¹ , C/2, 100 cycles, CR = 40%, CE = 90%	
	1-μm-thick TEOS-modified lithium	W modification: Li/Li battery: R _{CT} = 34 Ω, 20 cycles, 1 mA cm ⁻²	Umeda et al., 2011
		W/O modification: Li/Li battery: R _{CT} = 197 Ω, 10 cycles, 1 mA cm ⁻²	
	24-nm-thick hybrid silicate coating	W modification: LFP/Li battery: 104 mAh g ⁻¹ , C/2, 500 cycles, CR = 75%, CE = 99.87%	Liu et al., 2018
		W/O modification: LFP/Li battery: 77 mAh g ⁻¹ , C/2, 330 cycles, CR = 61%, CE = <60%	
	Cross-linkable silane and polymer layers on lithium	W modification: Li/Li battery: R _{overall} = 12 kΩ after assembling, solid-state LLZO electrolyte, 25°C. Stable cycling, >150 cycles, 0.1 mA cm ⁻² , 80°C	Delaporte et al., 2019
		W/O modification: Li/Li battery: R _{overall} = 550 kΩ after assembling, solid-state LLZO electrolyte, 25°C. Short-circuit, 33 cycles, 0.05 mA cm ⁻² , 80°C	
Mechanical modification	Micro-needle treatment	W modification: LFP/Li battery: 1 mAh, C/2, 150 cycles, CR = 85%	Ryou et al., 2015
		W/O modification: LFP/Li battery: 0.3 mAh, C/2, 150 cycles, CR = 26%	
	Pyramidal relief stamping	W modification: LMO/Li battery: 88.9 mAh g ⁻¹ , C/2, 450 cycles, CR = 88.7%	Park et al., 2016
		W/O modification: LMO/Li battery: 42.7 mAh g ⁻¹ , C/2, 250 cycles, CR = 42.7%	
	Roll-pressed lithium	W modification: Li/Li battery: R _{SEI} = 850 Ω, 1 cycle, 0.1 mA cm ⁻²	Becking et al., 2017
		W/O modification: Li/Li battery: R _{SEI} = 1,600 Ω, 1 cycle, 0.1 mA cm ⁻²	
SEI formation before reassembling	FEC-modified lithium	W modification: Li/Li battery: R _{CT} = 150 Ω, 60 h at OCV. Li/O ₂ battery = 1,000 mAh g ⁻¹ fixed, 300 mA g ⁻¹ , 2.0 V cutoff voltage, 31 cycles	Liu et al., 2015
		W/O modification: Li/Li battery: R _{CT} = 440 Ω, 60 h at OCV. Li/O ₂ battery = 1,000 mAh g ⁻¹ fixed, 300 mA g ⁻¹ , 2.0 V cutoff voltage, >100 cycles	
	Dual-layered film	W modification: Li/S battery: 891 mAh g ⁻¹ , 1C, 600 cycles, CR = 76%, CE = 98.6%	Cheng et al., 2016

(Continued)

TABLE 1 | Continued

Type of modification	Nature of modification	Best electrochemical improvement observed	References
		W/O modification: Li/S battery: 874 mAh g ⁻¹ , 1C, 600 cycles, CR = 39%, CE = 61%	
	LiAl alloy layer	W modification: Li/Li battery: CE = 99.5%, 50 cycles, 4 mA cm ⁻²	Ishikawa et al., 2005
		W/O modification: Li/Li battery: CE = 92.2%, 50 cycles, 4 mA cm ⁻²	
	LiAl alloy layer	W modification: Li/S battery: 844 mAh g ⁻¹ , C/2, 100 cycles, CR = 75%, CE = 92%	Ma et al., 2017
		W/O modification: Li/S battery: 790 mAh g ⁻¹ , C/2, 100 cycles, CR = 70%, CE = 83%	

ALD, Atomic layer deposition; CDC/S, Carbide derived-carbon/sulfur composite; CE, Coulombic efficiency; CR, Capacity retention; FEC, Fluoroethylene carbonate; FG, Fluorinated reduced graphene oxide; LCO, LiCoO₂; LFP, LiFePO₄; LMO, LiMn₂O₄; LiPON, Lithium phosphorous oxynitride; LTO, Li₄Ti₅O₁₂; MWCNT, Multiwall carbon nanotubes; NMC111, LiNi_{1/3}Co_{1/3}Mn_{1/3}O₂; NMC622, LiNi_{0.6}Co_{0.2}Mn_{0.2}O₂; OCV, Open-circuit voltage; OEGB, Oligo(ethylene glycol) borate; R_{CT}, Charge-transfer resistance; R_{el}, Electrolyte resistance; r-GO, Reduced graphene oxide; R_{overall}, Overall polarization resistance; R_{SEI}, Solid electrolyte interface resistance; SBR, Styrene-butadiene rubber; SC, Sulfurized carbon; SEI, Solid electrolyte interface; TEOS, Tetraethoxysilane; W, With; W/O, Without; ΔE, Polarization voltage.

only cycled for 31 cycles with the cutoff voltage restricted to 2.0 V, the battery made with protected lithium worked normally for more than 100 cycles. XRD analyses supported these results showing less LiOH (corrosion product) on the surface of modified lithium after cycling.

An electroplated implantable SEI made by pre-cycling Li metal in a LiTFSI-LiNO₃-Li₂S₅ ternary salt electrolyte was proposed by Cheng et al. (2016). The modified lithium was analyzed by XPS, revealing a composite layer made of organic species such as ROCO₂Li and ROLi and inorganic compounds like Li₃N, Li₂N_xO_y, LiF, Li₂S_x, and Li₂S_xO_y. This dual-layered film can easily restrict the formation of dendrites and protect the surface of lithium from electrolyte aggression. This was confirmed with cycling in a Li/S battery, where the cell with precycled lithium exhibited a high initial discharge capacity of 891 mAh g⁻¹ at a 1C rate, which corresponded to a capacity retention of 76% after 600 cycles. The cell made with pristine lithium had a low retention of ~39% from its initial capacity of 874 mAh g⁻¹. In addition, the Coulombic efficiency for the modified cell remained stable around 98.6% throughout the cycling whereas that of the reference cell decayed sharply from 93 to 61%. The high efficiency of the implantable SEI layer has been attributed to LiF and the balanced co-existence of Li₂S and Li₂S_xO_y in the protective film. These species render a highly functional SEI layer with superior ionic conductivity and electrical insulation.

Another example proposed to form a Li-Al alloy by cycling a lithium electrode in an electrolyte (1 M LiTFSI PC:DMC) containing a small amount of AlI₃ (600 ppm Al³⁺) (Ishikawa et al., 2005). The pre-treated lithium was then incorporated in a Li/Li symmetric cell with fresh electrolyte and cycled at a depth of discharge (DoD) of 2% at different current densities. After 50 cycles, average Coulombic efficiencies of 99.5 and 92.2% were obtained for the cells made with treated and pristine lithium electrodes, respectively. Unfortunately, no additional electrochemical tests in the full cell were presented to support these results. A couple of years later, Archer's research group reported a very similar example of Li-Al alloy electrochemically formed in 1 M LiTFSI DME:DOL also containing 600 ppm of

AlI₃ (Ma et al., 2017). The procedure led to the formation of a surface coating on Li that includes LiI, Li-Al, and a thin polymer film derived from the polymerization of DOL initiated by the Al³⁺ cation. The pristine and modified lithium were immersed for 12 h in a Li/S battery electrolyte and then characterized by XRD. It was found that the bare lithium strongly reacted with the electrolyte since the appearance of peaks attributed to the Li₂S crystal structure, which was not observed for AlI₃-modified lithium. A Li/stainless steel cell configuration was adopted to calculate the Coulombic efficiency of both the bare and modified lithium electrodes. Under a constant charge/discharge current of 2 mA cm⁻², average CEs of ~70 and 92% were obtained on 100 cycles for the pristine and the modified lithium electrodes, respectively. A long-cycling experiment over 100 cycles at a C/2 rate for a full Li/S battery showed better capacity retention with the modified anode and higher Coulombic efficiency (92 vs. 83% for pristine lithium). These improvements were attributed to the protection effect of the LiI/Li-Al/polymer layer from reaction with soluble polysulfides, therefore reducing the shuttling effect and anode surface passivation.

SUMMARY AND PROSPECTS

Lithium metal electrodes have been recently reconsidered as potential anodes for high-energy density batteries and especially for all-solid state batteries. However, due to safety concerns mainly caused by dendrite growth and possible fire hazards, surface protection of the metal is needed. Numerous strategies, including modified current collectors or separators, electrolyte additives, lithium composite anodes (that are not pure lithium in practice), or utilization of lithium powder instead of 2D lithium foil, have been considered. Most of these techniques are not transferable to an industrial scale or are too expensive. These aspects motivated us to compile the research studies focused on the surface modification of 2D lithium foil because it represents the easiest way to produce industrial quantities of treated lithium directly on the production line.

We divided the different surface treatments into 12 categories (Table 1). Among them, sputtering and ALD methods are limited

to the laboratory scale, although they led to very thin coatings on lithium surfaces and remarkable improvements in the batteries. They are particularly interesting for pure academic researches to put in evidence the impact of nanometric deposition of well-organized organic/inorganic layers. Similarly, the preformation of artificial SEI on lithium surface by electrochemistry is of interest to understand mechanisms of passivation and the effect of salts, solvents or additives used on the electrochemical performance. Unfortunately, from an industrial point of view, this technique must be dismissed as well as ALD and sputtering methods due to their high prices and because they are hardly transposable to industrial scale. Polymer coatings with and without charges is a well-known method consisting of preparing a slurry that is spread on the surface of the material to coat it via the so-called web coating method. According to us, this is one of the methods to explore for efficient protection of lithium anode and particularly to increase its contact with ceramic in all-solid state batteries, as we recently showed (Kozen et al., 2015). Moreover, this method is cost effective and already widely used to produce Li-ion cathodes and anodes. Other economical methods like dip coating or spray coating can be also used to yield thin films on lithium surface. Spontaneous reactions with lithium in gas or liquid phases (including silane chemistry) are possible ways to rapidly produce low-cost treated lithium metal foil as long as one side of lithium is modified to ensure good electrical contact on the other side. With the paint-roller technique or the dipping method, passivation can be easily achieved during lithium foil formation. Carbon deposition on the lithium surface by spontaneous reactions or by applying a self-standing carbon film is an ingenious method to redistribute the lithium flux and to impede dendrite formation. However, in addition to time for film preparation, the price of carbons such as graphene and carbon nanotubes severely limits the scaling of this method for

the moment. Furthermore, the high electrical conductivity of these films can promote side reactions at the electrode/electrolyte interface. Finally, the few examples of mechanical modification of lithium seem very promising due to the ease and low price of the method. A designed roll with micro-patterns directly placed on the production line can yield high amount of modified-lithium with good homogeneity and reproducibility that is an important factor for industrials. The increase in initial specific surface area clearly reduces the actual current density of the Li metal battery and thus the formation of dendrites. However, for all-solid state batteries, intimate contact between electrodes and electrolyte is needed, and by consequence, this technique is compatible with liquid electrolytes and probably represents an option with solid polymer electrolyte.

Only a few examples of pre-treatment of lithium foil for direct use in all-solid-state batteries have been reported. This review proposes different methods and chemistries to investigate in the future for making lithium anodes safer, which will accelerate the arrival of all-solid-state batteries on the market that are believed to be the future of electrochemical energy storage. With this aim, the modification method will have to be reproducible, safe, and transferable to the industrial level, and cost-effective to be widely developed.

AUTHOR CONTRIBUTIONS

All authors listed have made a substantial, direct and intellectual contribution to the work, and approved it for publication.

ACKNOWLEDGMENTS

Éloïse Leroux is graciously thanked for the design of the sketch in the introduction part.

REFERENCES

- Agrawal, R. C., and Pandey, G. P. (2008). Solid polymer electrolytes: materials designing and all-solid-state battery applications: an overview. *J. Phys. D Appl. Phys.* 41:223001. doi: 10.1088/0022-3727/41/22/223001
- Akridge, J. R., and Vourlis, H. (1986). Solid state batteries using vitreous solid electrolytes. *Solid State Ion* 18–19, 1082–1087. doi: 10.1016/0167-2738(86)90313-9
- Aurbach, D., Zinigrad, E., Teller, H., and Dan, P. (2000). Factors which limit the cycle life of rechargeable lithium (metal) batteries. *J. Electrochem. Soc.* 147, 1274–1279. doi: 10.1149/1.1393349
- Bai, M., Xie, K., Yuan, K., Zhang, K., Li, N., Shen, C., et al. (2018). A scalable approach to dendrite-free lithium anodes via spontaneous reduction of spray-coated graphene oxide layers. *Adv. Mater.* 30:1801213. doi: 10.1002/adma.201801213
- Basile, A., Bhatt, A. I., and O'Mullane, A. P. (2016). Stabilizing lithium metal using ionic liquids for long-lived batteries. *Nat. Commun.* 7:ncomms11794. doi: 10.1038/ncomms11794
- Becking, J., Gröbmeyer, A., Kolek, M., Rodehorst, U., Schulze, S., Winter, M., et al. (2017). Lithium-metal foil surface modification: an effective method to improve the cycling performance of lithium-metal batteries. *Adv. Mater. Interfaces.* 4:1700166. doi: 10.1002/admi.201700166
- Belov, D. G., Yarmolenko, O. V., Peng, A., and Efimov, O. N. (2006). Lithium surface protection by polyacetylene in situ polymerization. *Synth. Met.* 156, 745–751. doi: 10.1016/j.synthmet.2006.04.006
- Bobnar, J., Lozinšek, M., Kapun, G., Njel, C., Dedryvère, R., Genorio, B., et al. (2018). Fluorinated reduced graphene oxide as a protective layer on the metallic lithium for application in the high energy batteries. *Sci. Rep.* 8:5819. doi: 10.1038/s41598-018-23991-2
- Bouchet, R. (2014). A stable lithium metal interface. *Nat. Nanotech.* 9, 572–573. doi: 10.1038/nnano.2014.165
- Buonaiuto, M., Neuhold, S., Schroeder, D. J., Lopez, C. M., and Vaughey, J. T. (2015). Functionalizing the surface of lithium-metal anodes. *ChemPlusChem* 80, 363–367. doi: 10.1002/cplu.201402084
- Cha, E., Patel, M. D., Park, J., Hwang, J., Prasad, V., Cho, K., et al. (2018). 2D MoS₂ as an efficient protective layer for lithium metal anodes in high-performance Li-S batteries. *Nat. Nanotechnol.* 13, 337–344. doi: 10.1038/s41565-018-0061-y
- Cheng, X.-B., Yan, C., Chen, X., Guan, C., Huang, J.-Q., H., Peng, J., et al. (2016). Implantable Solid electrolyte interphase in lithium-metal batteries. *Chem* 1, 287–297. doi: 10.1016/j.chempr.2017.01.003
- Choi, N.-S., Lee, Y. M., Cho, K. Y., Ko, D.-H., and Park, J.-K. (2004b). Protective layer with oligo(ethylene glycol) borate anion receptor for lithium metal electrode stabilization. *Electrochem. Commun.* 6, 1238–1242. doi: 10.1016/j.elecom.2004.09.023
- Choi, N.-S., Lee, Y. M., Seol, W., Lee, J. A., and Park, J.-K. (2004a). Protective coating of lithium metal electrode for interfacial enhancement with gel polymer electrolyte. *Solid State Ion* 172, 19–24. doi: 10.1016/j.ssi.2004.05.008
- Choi, S. M., Kang, I. S., Sun, Y.-K., Song, J.-H., Chung, S.-M., and Kim, D.-W. (2013). Cycling characteristics of lithium metal batteries assembled

- with a surface modified lithium electrode. *Power Sources J.* 244, 363–368. doi: 10.1016/j.jpowsour.2012.12.106
- Choudhury, S., Tu, Z., Stalin, S., Vu, D., Fawole, K., Gunceler, D., et al. (2017). Electroless formation of hybrid lithium anodes for fast interfacial ion transport. *Angew. Chem. Int. Ed.* 56, 13070–13077. doi: 10.1002/anie.201707754
- Chung, K.-I., Kim, W.-S., and Choi, Y.-K. (2004). Lithium phosphorous oxynitride as a passive layer for anodes in lithium secondary batteries. *J. Electroanal. Chem.* 566, 263–267. doi: 10.1016/j.jelechem.2003.11.035
- Dahn, J. R., Fong, R., and Spoon, M. J. (1990). Suppression of staging in lithium-intercalated carbon by disorder in the host. *Phys. Rev. B* 42, 6424–6432. doi: 10.1103/PhysRevB.42.6424
- Delaporte, N., Guerfi, A., Demers, H., Lorrmann, H., Paoletta, A., and Zaghbi, K. (2019). Facile protection of lithium metal for all-solid-state batteries. *Chem Open.* 8, 192–195. doi: 10.1002/open.201900021
- Fan, L., Zhuang, H. L., Gao, L., Lu, Y., and Archer, L. A. (2017). Regulating Li deposition at artificial solid electrolyte interphases. *J. Mater. Chem. A* 5, 3483–3492. doi: 10.1039/C6TA10204B
- Fong, R., Von Sacken, U., and Dahn, J. R. (1990). Studies of lithium intercalation into carbons using nonaqueous electrochemical cells. *J. Electrochem. Soc.* 137, 2009–2013. doi: 10.1149/1.2086855
- Fu, K. K., Gong, Y., Fu, Z., Xie, H., Yao, Y., Liu, B., et al. (2017). Transient behavior of the metal interface in lithium metal–garnet batteries. *Angew. Chem. Int. Ed.* 56, 14942–14947. doi: 10.1002/anie.201708637
- Hu, Z., Zhang, S., Dong, S., Li, W., Li, H., Cui, G., et al. (2017). Poly(ethyl α -cyanoacrylate)-based artificial solid electrolyte interphase layer for enhanced interface stability of Li metal anodes. *Chem. Mater.* 29, 4682–4689. doi: 10.1021/acs.chemmater.7b00091
- Ishikawa, M., Kawasaki, H., Yoshimoto, N., and Morita, M. (2005). Pretreatment of Li metal anode with electrolyte additive for enhancing Li cycleability. *Power Sources J.* 146, 199–203. doi: 10.1016/j.jpowsour.2005.03.007
- Jia, W., Wang, Q., Yang, J., Fan, C., Wang, L., and Li, J. (2017). Pretreatment of lithium surface by using iodic acid (HIO₃) to improve its anode performance in lithium batteries. *ACS Appl. Mater. Interfaces* 9, 7068–7074. doi: 10.1021/acsami.6b14614
- Jing, H.-K., Kong, L.-L., Liu, S., Li, G.-R., and Gao, X.-P. (2015). Protected lithium anode with porous Al₂O₃ layer for lithium–sulfur battery. *J. Mater. Chem. A* 3, 12213–12219. doi: 10.1039/C5TA01490E
- Kang, I. S., Lee, Y.-, and S., Kim, D.-W. (2014). Improved cycling stability of lithium electrodes in rechargeable lithium batteries. *J. Electrochem. Soc.* 161, A53–A57. doi: 10.1149/2.029401jes
- Kazyak, E., Wood, K. N., and Dasgupta, N. P. (2015). Improved cycle life and stability of lithium metal anodes through ultrathin atomic layer deposition surface treatments. *Chem. Mater.* 27, 6457–6462. doi: 10.1021/acs.chemmater.5b02789
- Kim, H., Lee, J. T., Lee, D.-C., Oschatz, M., Cho, W. I., et al. (2013). Enhancing performance of Li–S cells using a Li–Al alloy anode coating. *Electrochem. Commun.* 36, 38–41. doi: 10.1016/j.elecom.2013.09.002
- Kim, K. H., Iriyama, Y., Yamamoto, K., Kumazaki, S., Asaka, T., Tanabe, K., et al. (2011). Characterization of the interface between LiCoO₂ and Li₇La₃Zr₂O₁₂ in an all-solid-state rechargeable lithium battery. *Power Sources J.* 196, 764–767. doi: 10.1016/j.jpowsour.2010.07.073
- Kozan, A. C., Lin, C.-F., Pearse, A. J., Schroeder, M. A., Han, X., Hu, L., et al. (2015). Next-generation lithium metal anode engineering via atomic layer deposition. *ACS Nano* 9, 5884–5892. doi: 10.1021/acsnano.5b02166
- Lee, D. J., Lee, H., Song, J., Ryou, M.-H., Lee, Y. M., Kim, H.-T., et al. (2014). Composite protective layer for Li metal anode in high-performance lithium–oxygen batteries. *Electrochem. Commun.* 40, 45–48. doi: 10.1016/j.elecom.2013.12.022
- Lee, Y. M., Choi, N.-S., Park, J. H., and Park, J.-K. (2003). Electrochemical performance of lithium/sulfur batteries with protected Li anodes. *Power Sources J.* 119–121, 964–972. doi: 10.1016/S0378-7753(03)00300-8
- Li, N.-W., Shi, Y., Yin, Y.-X., Zeng, X.-X., Li, J.-Y., Li, C.-J., et al. (2018). A flexible solid electrolyte interphase layer for long-life lithium metal anodes. *Angew. Chem. Int. Ed.* 57, 1505–1509. doi: 10.1002/anie.201710806
- Li, N.-W., Yin, Y.-X., Yang, C.-P., and Guo, Y.-G. (2016). An artificial solid electrolyte interphase layer for stable lithium metal anodes. *Adv. Mater.* 28, 1853–1858. doi: 10.1002/adma.201504526
- Li, Q., Sun, H. Y., Takeda, Y., Imanishi, N., Yang, J., and Yamamoto, O. (2001). Interface properties between a lithium metal electrode and a poly(ethylene oxide) based composite polymer electrolyte. *Power Sources J.* 94, 201–205. doi: 10.1016/S0378-7753(00)00587-5
- Liang, X., Pang, Q., Kochetkov, I. R., Sempere, M. S., Huang, H., Sun, X., et al. (2017). A facile surface chemistry route to a stabilized lithium metal anode. *Nat. Energy.* 2:17119. doi: 10.1038/nenergy.2017.119
- Lin, D., Liu, Y., Chen, W., Zhou, G., Liu, K., Dunn, B., et al. (2017b). Conformal lithium fluoride protection layer on three-dimensional lithium by nonhazardous gaseous reagent freon. *Nano Lett.* 17, 3731–3737. doi: 10.1021/acs.nanolett.7b01020
- Lin, D., Liu, Y., and Cui, Y. (2017a). Reviving the lithium metal anode for high-energy batteries. *Nat. Nanotech.* 12, 194–206. doi: 10.1038/nnano.2017.16
- Liu, F., Xiao, Q., Wu, H. B., Shen, L., Xu, D., Cai, M., et al. (2018). Fabrication of hybrid silicate coatings by a simple vapor deposition method for lithium metal anodes. *Adv. Energy Mater.* 8:1701744. doi: 10.1002/aenm.201701744
- Liu, Q.-C., Xu, J.-J., Yuan, S., Chang, Z.-W., Xu, D., Yin, Y.-B., et al. (2015). Artificial protection film on lithium metal anode toward long-cycle-life lithium–oxygen batteries. *Adv. Mater.* 27, 5241–5247. doi: 10.1002/adma.201501490
- Liu, Y., Lin, D., Yuen, P. Y., Liu, K., Xie, J., Dauskardt, R. H., et al. (2017). An artificial solid electrolyte interphase with high Li-ion conductivity, mechanical strength, and flexibility for stable lithium metal anodes. *Adv. Mater.* 29, 1605531. doi: 10.1002/adma.201605531
- Ma, G., Wen, Z., Wang, Q., Shen, C., Jin, J., and Wu, X. (2014a). Enhanced cycle performance of a Li–S battery based on a protected lithium anode. *J. Mater. Chem. A* 2, 19355–19359. doi: 10.1039/C4TA04172K
- Ma, G., Wen, Z., Wu, M., Shen, C., Wang, Q., Jin, J., et al. (2014b). Lithium anode protection guided highly-stable lithium–sulfur battery. *Chem. Commun.* 50, 14209–14212. doi: 10.1039/C4CC05535G
- Ma, L., Kim, M. S., and Archer, L. A. (2017). Stable artificial solid electrolyte interphases for lithium batteries. *Chem. Mater.* 29, 4181–4189. doi: 10.1021/acs.chemmater.6b03687
- Marchioni, F., Star, K., Menke, E., Buffeteau, T., Servant, L., Dunn, B., et al. (2007). Protection of lithium metal surfaces using chlorosilanes. *Langmuir* 23, 11597–11602. doi: 10.1021/la701662r
- Neuhold, S., Schroeder, D. J., and Vaughey, J. T. (2012). Effect of surface preparation and R-group size on the stabilization of lithium metal anodes with silanes. *Power Sources J.* 206, 295–300. doi: 10.1016/j.jpowsour.2012.01.129
- Neuhold, S., Vaughey, J. T., Grogger, C., and López, C. M. (2014). Enhancement in cycle life of metallic lithium electrodes protected with Fp-silanes. *Power Sources J.* 254, 241–248. doi: 10.1016/j.jpowsour.2013.12.057
- Notten, P. H. L., Roozeboom, F., Niessen, R. A. H., and Baggetto, L. (2007). 3-D integrated all-solid-state rechargeable batteries. *Adv. Mater.* 19, 4564–4567. doi: 10.1002/adma.200702398
- Odziemkowski, M., and Irish, D. E. (1992). An electrochemical study of the reactivity at the lithium electrolyte/bare lithium metal interface: I. Purified electrolytes. *J. Electrochem. Soc.* 139, 3063–3074. doi: 10.1149/1.2069033
- Odziemkowski, M., and Irish, D. E. (1993). An electrochemical study of the reactivity at the lithium electrolyte/bare lithium metal interface: II. Unpurified solvents. *J. Electrochem. Soc.* 140, 1546–1555. doi: 10.1149/1.2221600
- Paoletta, A., Demers, H., Chevallier, P., Gagnon, C., Girard, G., Delaporte, N., et al. (2019). A platinum nanolayer on lithium metal as an interfacial barrier to shuttle effect in Li–S batteries. *Power Sources J.* 427, 201–206. doi: 10.1016/j.jpowsour.2019.04.078
- Park, J., Jeong, J., Lee, Y., Oh, M., Ryou, M.-H., and Lee, Y. M. (2016). Micro-patterned lithium metal anodes with suppressed dendrite formation for post lithium-ion batteries. *Adv. Mater. Interfaces.* 3:1600140. doi: 10.1002/admi.201600140
- Peng, Z., Wang, S., Zhou, J., Jin, Y., Liu, Y., Qin, Y., et al. (2016). Volumetric variation confinement: surface protective structure for high cyclic stability of lithium metal electrodes. *J. Mater. Chem. A* 4, 2427–2432. doi: 10.1039/C5TA10050J
- Ryou, M.-H., Lee, Y. M., Lee, Y., Winter, M., and Bieker, P. (2015). Mechanical surface modification of lithium metal: towards improved Li metal anode performance by directed Li plating. *Adv. Funct. Mater.* 25, 834–841. doi: 10.1002/adfm.201402953

- Salvatierra, R. V., López-Silva, G. A., Jalilov, A. S., Yoon, J., Wu, G., Tsai, A.-L., et al. (2018). Suppressing Li metal dendrites through a solid Li-ion backup layer. *Adv. Mater.* 30:1803869. doi: 10.1002/adma.201803869
- Stone, G. M., Mullin, S. A., Teran, A. A., Hallinan, D. T., Minor, A. M., Hexemer, A., et al. (2012). Resolution of the modulus versus adhesion dilemma in solid polymer electrolytes for rechargeable lithium metal batteries. *J. Electrochem. Soc.* 159, A222–A227. doi: 10.1149/2.030203jes
- Sudo, R., Nakata, Y., Ishiguro, K., Matsui, M., Hirano, A., Takeda, Y., et al. (2014). Interface behavior between garnet-type lithium-conducting solid electrolyte and lithium metal. *Solid State Ion* 262, 151–154. doi: 10.1016/j.ssi.2013.09.024
- Tang, W., Yin, X., Kang, S., Chen, Z., Tian, B., Teo, S. L., et al. (2018). Lithium silicide surface enrichment: a solution to lithium metal battery. *Adv. Mater.* 30, 1801745. doi: 10.1002/adma.201801745
- Tarascon, J.-M., and Armand, M. (2001). Issues and challenges facing rechargeable lithium batteries. *Nature* 414, 359–367. doi: 10.1038/35104644
- Thompson, R. S., Schroeder, D. J., López, C. M., Neuhold, S., and Vaughey, J. T. (2011). Stabilization of lithium metal anodes using silane-based coatings. *Electrochem. Commun.* 13, 1369–1372. doi: 10.1016/j.elecom.2011.08.012
- Umeda, G. A., Menke, E., Richard, M., Stamm, K. L., Wudl, F., and Dunn, B. (2011). Protection of lithium metal surfaces using tetraethoxysilane. *J. Mater. Chem.* 21, 1593–1599. doi: 10.1039/C0JM02305A
- Wang, G., Xiong, X., Xie, D., Fu, X., Lin, Z., Yang, C., et al. (2019). A scalable approach for dendrite-free alkali metal anodes via room-temperature facile surface fluorination. *ACS Appl. Mater. Interfaces* 11, 4962–4968. doi: 10.1021/acsami.8b18101
- Wang, L., Wang, Q., Jia, W., Chen, S., Gao, P., and Li, J. (2017). Li metal coated with amorphous Li_3PO_4 via magnetron sputtering for stable and long-cycle life lithium metal batteries. *Power Sources J.* 342, 175–182. doi: 10.1016/j.jpowsour.2016.11.097
- Wang, L., Zhang, L., Wang, Q., Li, W., Wu, B., Jia, W., et al. (2018). Long lifespan lithium metal anodes enabled by Al_2O_3 sputter coating. *Energy Storage Mater.* 10, 16–23. doi: 10.1016/j.ensm.2017.08.001
- Wu, M., Wen, Z., Jin, J., and Chowdari, B. V. (2016). Trimethylsilyl chloride-modified Li anode for enhanced performance of Li-S cells. *ACS Appl. Mater. Interfaces* 8, 16386–16395. doi: 10.1021/acsami.6b02612
- Wu, M., Wen, Z., Liu, Y., Wang, X., and Huang, L. (2011). Electrochemical behaviors of a Li_3N modified Li metal electrode in secondary lithium batteries. *Power Sources J.* 196, 8091–8097. doi: 10.1016/j.jpowsour.2011.05.035
- Xu, W., Wang, J., Ding, F., Chen, X., Nasybulin, E., Zhang, Y., et al. (2014). Lithium metal anodes for rechargeable batteries. *Energy Environ. Sci.* 7, 513–537. doi: 10.1039/C3EE40795K
- Yan, C., Cheng, X.-B., Tian, Y., Chen, X., Zhang, X.-Q., Li, W.-J., et al. (2018). Dual-layered film protected lithium metal anode to enable dendrite-free lithium deposition. *Adv. Mater.* 30:1707629. doi: 10.1002/adma.201707629
- Yazami, R., and Touzain, P. (1983). A reversible graphite-lithium negative electrode for electrochemical generators. *Power Sources J.* 9, 365–371. doi: 10.1016/0378-7753(83)87040-2
- Zhamu, A., Chen, G., Liu, C., Neff, D., Fang, Q., Yu, Z., et al. (2012). Reviving rechargeable lithium metal batteries: enabling next-generation high-energy and high-power cells. *Energy Environ. Sci.* 5, 5701–5707. doi: 10.1039/C2EE02911A
- Zhang, Y.-J., Xia, X.-H., Wang, D.-H., Wang, X.-L., Gu, C.-D., and Tu, J.-P. (2016b). Integrated reduced graphene oxide multilayer/Li composite anode for rechargeable lithium metal batteries. *RSC Adv.* 6, 11657–11664. doi: 10.1039/C5RA25553H
- Zhang, Y.-J., Xia, X.-H., Wang, X.-L., Gu, C.-D., and Tu, J.-P. (2016a). Graphene oxide modified metallic lithium electrode and its electrochemical performances in lithium-sulfur full batteries and symmetric lithium-metal coin cells. *RSC Adv.* 6, 66161–66168. doi: 10.1039/C6RA13039A
- Zhang, Y. J., Liu, X. Y., Bai, W. Q., Tang, H., Shi, S. J., Wang, X. L., et al. (2014). Magnetron sputtering amorphous carbon coatings on metallic lithium: towards promising anodes for lithium secondary batteries. *Power Sources J.* 266, 43–50. doi: 10.1016/j.jpowsour.2014.04.147
- Zhao, J., Liao, L., Shi, F., Lei, T., Chen, G., Pei, A., et al. (2017). Surface fluorination of reactive battery anode materials for enhanced stability. *J. Am. Chem. Soc.* 139, 11550–11558. doi: 10.1021/jacs.7b05251
- Zheng, G., Lee, S. W., Liang, Z., Lee, H.-W., Yan, K., Yao, H., et al. (2014). Interconnected hollow carbon nanospheres for stable lithium metal anodes. *Nat Nanotechnol.* 9, 618–623. doi: 10.1038/nnano.2014.152

Conflict of Interest: ND, YW, and KZ were employed by the company Hydro-Québec.

Copyright © 2019 Delaporte, Wang and Zaghbi. This is an open-access article distributed under the terms of the Creative Commons Attribution License (CC BY). The use, distribution or reproduction in other forums is permitted, provided the original author(s) and the copyright owner(s) are credited and that the original publication in this journal is cited, in accordance with accepted academic practice. No use, distribution or reproduction is permitted which does not comply with these terms.